

**SOUND TRANSMISSION BEHAVIOUR, FIRE  
RESISTING PROPERTIES AS WELL AS  
STRUCTURAL PERFORMANCE OF FULL  
SCALE RUBBERIZED LIGHTWEIGHT FOAMED  
CONCRETE USING MAGNESIUM OXIDE  
BOARD AS THE SKIN LAYER**

**NG KEE SIANG**

**UNIVERSITI TUNKU ABDUL RAHMAN**

**SOUND TRANSMISSION BEHAVIOUR, FIRE RESISTING  
PROPERTIES AS WELL AS STRUCTURAL PERFORMANCE OF  
FULL SCALE RUBBERIZED LIGHTWEIGHT FOAMED CONCRETE  
USING MAGNESIUM OXIDE BOARD AS THE SKIN LAYER**

**NG KEE SIANG**

**A project report submitted in partial fulfilment of the  
requirements for the award of  
Bachelor of Civil Engineering with Honours**

**Lee Kong Chian Faculty of Engineering and Science  
Universiti Tunku Abdul Rahman**

**May 2023**

**DECLARATION**

I hereby declare that this project report is based on my original work except for citations and quotations which have been duly acknowledged. I also declare that it has not been previously and concurrently submitted for any other degree or award at UTAR or other institutions.

Signature : Siang

Name : NG KEE SIANG

ID No. : 18UEB03851

Date : 28 APRIL 2023

**APPROVAL FOR SUBMISSION**

I certify that this project report entitled **SOUND TRANSMISSION BEHAVIOUR, FIRE RESISTING PROPERTIES AS WELL AS STRUCTURAL PERFORMANCE OF FULL SCALE RUBBERIZED LIGHTWEIGHT FOAMED CONCRETE USING MAGNESIUM OXIDE BOARD AS THE SKIN LAYER** was prepared by **NG KEE SIANG** has met the required standard for submission in partial fulfilment of the requirements for the award of Bachelor of Civil Engineering with Honours at Universiti Tunku Abdul Rahman.

Approved by,



Signature : \_\_\_\_\_

Supervisor : Ts. Dr Lee Foo Wei  
\_\_\_\_\_

Date : 28 APRIL 2023  
\_\_\_\_\_

Signature : \_\_\_\_\_

Co-Supervisor : \_\_\_\_\_

Date : \_\_\_\_\_

The copyright of this report belongs to the author under the terms of the copyright Act 1987 as qualified by Intellectual Property Policy of Universiti Tunku Abdul Rahman. Due acknowledgement shall always be made of the use of any material contained in, or derived from, this report.

© 2023, Ng Kee Siang. All right reserved.

## ACKNOWLEDGEMENTS

I want to thank everyone who contributed to the successful completion of this project. First and foremost, I would like to express my sincere gratitude to my research supervisor, Ts. Dr Lee Foo Wei, for allowing me to participate in and conduct this research study. I am glad to complete this study under his fruitful advice, patient guidance, and full support throughout the research development.

In addition, I wish to express my gratitude to Mr Lim Zhi Heng, Mr Mok Shao Jun, Mr Loh Yong Wei, and Mr Jason Ting Jing Cheng for their support and assistance during the research development. Furthermore, I want to thank my fellow senior coursemates for their experience sharing throughout the research development. Besides, I also wish to express a thank you note to Dr Lim Jee Hock and the lab officers for their assistance during the specimen laboratory testing.

Last, I would like to thank my loving parents and friends who helped and encouraged me throughout the research.

## ABSTRACT

In Malaysia, the generation of waste tyres is a significant environmental problem, with approximately 8.2 million waste tyres generated annually. To address this issue, this study investigates the potential of rubberized lightweight foamed concrete with the skin layers of magnesium oxide board as a sandwiched wall panel system. First, crumb rubber ground from the waste tyre is incorporated into the concrete mixture at 80 % replacement, producing a fresh density of 1150 kg/m<sup>3</sup>. Then, sandwiched wall panels are fabricated from this material by adhesively connecting the rubberized lightweight foamed concrete core to the magnesium oxide board as the skin layers using an adhesive agent. After the fabrication of sandwiched wall panel, four different product and laboratory tests are conducted to evaluate its engineering properties. The Sound Reduction Index (SRI) is determined as 43 dB indicating the ability of the sandwiched wall panel to sound absorption. Besides, the sandwiched wall panel also passes the 2-hour fire resistance rating test and 2.5-minute hose stream test. This essential information indicates the durability of the sandwiched wall panel in adverse conditions such as prolonged exposure to a high-temperature fire scene and the high pressure of the hose stream exerted on it. In addition, the flexural strength test conducted on the sandwiched wall panel also evaluates its Modulus of Rupture (MOR) to meet the standard requirements with a minimum value of 1.5 MPa. The MOR evaluated is 2.2313 MPa for the sandwiched wall panel, and it is fulfilling the standard requirements. In conclusion, this study demonstrates the potential of the rubberized lightweight foamed concrete with the skin layers of magnesium oxide board as a sandwiched wall panel for commercialisation in the construction industry. The engineering properties of the sandwiched wall panel were favourable, with high sound absorption, good fire resistance rating, and sufficient flexural strength, making it suitable for non-load-bearing wall panel applications. Last but not least, this study also contributes to waste tyre management, extends the life cycle of rubber tyres, and promotes sustainable construction practices, namely Industrialised Building System (IBS) and Green Building Index (GBI).

## TABLE OF CONTENTS

<b>ACKNOWLEDGEMENTS</b>		<b>iv</b>
<b>ABSTRACT</b>		<b>v</b>
<b>TABLE OF CONTENTS</b>		<b>vi</b>
<b>LIST OF TABLES</b>		<b>ix</b>
<b>LIST OF FIGURES</b>		<b>x</b>
<b>LIST OF SYMBOLS / ABBREVIATIONS</b>		<b>xii</b>
<b>CHAPTER</b>		
<b>1</b>	<b>INTRODUCTION</b>	<b>1</b>
1.1	General Introduction	1
1.2	Importance of the Study	2
1.3	Problem Statement	4
1.4	Aim and Objectives	5
1.5	Scope and Limitation of the Study	6
1.6	Contribution of the Study	7
1.7	Outline of the Report	8
<b>2</b>	<b>LITERATURE REVIEW</b>	<b>9</b>
2.1	Introduction	9
2.2	Types of Lightweight Concrete	9
2.2.1	Lightweight Aggregate Concrete	9
2.2.2	No Fines Concrete	10
2.2.3	Aerated Concrete	11
2.2.4	Lightweight Foamed Concrete	11
2.3	Rubberized Lightweight Foamed Concrete	12
2.4	Types of Rubber Aggregates	13
2.4.1	Chipped Rubber	13
2.4.2	Crumb Rubber	13
2.4.3	Ground Rubber	14
2.5	Application of Crumb Rubber	14



2.6	Fresh Properties of Rubberized Lightweight Foamed Concrete	15
2.6.1	Workability	15
2.7	Hardened Properties of Rubberized Lightweight Foamed Concrete	16
2.7.1	Density	16
2.7.2	Compressive Strength	18
2.7.3	Flexural Strength	19
2.7.4	Fire Performance	20
2.7.5	Thermal Properties	21
2.7.6	Acoustics Properties	22
2.8	Sandwiched Wall Panel	24
2.9	Magnesium Oxide Board	25
2.10	Summary	25
<b>3</b>	<b>METHODOLOGY AND WORK PLAN</b>	<b>26</b>
3.1	Introduction	26
3.2	Raw Materials Preparation	27
3.2.1	Ordinary Portland Cement	27
3.2.2	Fine Aggregate	28
3.2.3	Crumb Rubber	28
3.2.4	Water	29
3.2.5	Foaming Agent	29
3.2.6	Magnesium Oxide Board	30
3.2.7	TPS Thin Bed Adhesive Premium 668	30
3.3	Mix Ratio for Rubberized Lightweight Foamed Concrete	31
3.4	Concrete Mixing	32
3.5	Concrete Casting	33
3.6	Concrete Curing	34
3.7	Skin Layer Installation	34
3.8	Acoustic Insulation Test	35
3.9	Fire Resistance Rating Test	36
3.10	Hose Stream Test	37
3.11	Flexural Strength Test	38

	3.12	Summary	39
<b>4</b>		<b>RESULTS AND DISCUSSION</b>	<b>40</b>
	4.1	Introduction	40
	4.2	Acoustic Insulation Test	41
	4.3	Fire Resistance Rating Test	45
		4.3.1 Integrity	48
		4.3.2 Insulation	53
	4.4	Hose Stream Test	59
	4.5	Flexural Strength Test	61
	4.6	Summary	65
<b>5</b>		<b>CONCLUSIONS AND RECOMMENDATIONS</b>	<b>66</b>
	5.1	Conclusions	66
	5.2	Recommendations for future work	67
		<b>REFERENCES</b>	<b>68</b>

**LIST OF TABLES**

Table 2.1:	Minimum LFC Thickness for a Different Level of Fire Resistance Rating (Othuman and Wang, 2011).	20
Table 2.2:	Noise Reduction Coefficient for a Different Type of Concrete with Different Crumb Rubber Content (Sukontasukkul, 2009).	23
Table 3.1:	Specimen Mix Ratio.	31
Table 4.1:	Sound Reduction Index (SRI) at Different Frequencies.	44
Table 4.2:	Deflection Measured at Five Measuring Points.	50
Table 4.3:	Temperature Measured at Seven Thermocouples.	56
Table 4.4:	Temperature Rise at the Unexposed Surface at a 10-minute Interval.	58
Table 4.5:	Load-deflection Information for Sandwiched Wall Panel.	64

## LIST OF FIGURES

Figure 3.1:	Flowchart of Methodology.	26
Figure 3.2:	ORANG KUAT Ordinary Portland Cement (OPC).	27
Figure 3.3:	Powdered Crumb Rubber.	28
Figure 3.4:	TPS Thin Bed Adhesive Premium 668.	30
Figure 3.5:	Concrete Mixing Process.	32
Figure 3.6:	Concrete Casting Process.	33
Figure 3.7:	Concrete Curing Process.	34
Figure 4.1:	Test Setup for Testing of Sandwiched Wall Panel in the Source Room.	41
Figure 4.2:	Test Setup for Testing the Sandwiched Wall Panel in the Receiving Room.	42
Figure 4.3:	Graph on Sound Reduction Index (SRI) versus Frequencies.	43
Figure 4.4:	The Exposed Face of the Sandwiched Wall Panel Before the Test.	46
Figure 4.5:	The Exposed Face of the Sandwiched Wall Panel After the Test.	46
Figure 4.6:	The Unexposed Face of the Sandwiched Wall Panel Before the Test.	47
Figure 4.7:	The Unexposed Face of the Sandwiched Wall Panel After the Test.	47
Figure 4.8:	Location of Points A to E for Deflection Measuring.	49
Figure 4.9:	Graph on Deflection versus Time at Five Measuring Points.	49
Figure 4.10:	General Arrangement of the Concrete Core.	51
Figure 4.11:	General Arrangement of the Magnesium Oxide Board.	52
Figure 4.12:	Location of Thermocouple No.1 to 7.	53

Figure 4.13: Graph on Temperature versus Time at Seven Thermocouples.	55
Figure 4.14: Graph on Rise in Mean Temperature versus Time.	57
Figure 4.15: Graph on Rise in Maximum Temperature versus Time.	57
Figure 4.16: The Exposed Face of the Specimen after the Hose Stream Test.	60
Figure 4.17: Actual Set-up of Flexural Strength Test.	61
Figure 4.18: Specimen's Condition at Ultimate Failure.	62
Figure 4.19: Load-deflection Curve for Sandwiched Wall Panel.	64

## LIST OF SYMBOLS / ABBREVIATIONS

$\alpha$	Sound absorption coefficient, %
$A$	Sound absorption area in receiving chamber, m <sup>2</sup>
$B$	Average width of the specimen, mm
$D$	Average depth of specimen, mm
$K$	Thermal conductivity
$L$	Span length, mm
$L_1$	Average sound pressure level in source chamber, dB
$L_2$	Average sound pressure level in receiving chamber, dB
$P$	Maximum applied load indicated by the testing machine, kN
$R$	Modulus of Rupture
$R_w$	Sound Reduction Index
$S$	Area of test specimen, m <sup>2</sup>
ASTM	American Society for Testing and Materials
BS	British Standard
CRMA	Crumb Rubber Modified Asphalt
CSH	Calcium Silicate Hydrate
GBI	Green Building Index
IBS	Industrialised Building System
ISO	International Organisation for Standardization
ITZ	Interfacial Transition Zone
LFC	Lightweight Foamed Concrete
LVDT	Linear Voltage Displacement Transducer
MOR	Modulus of Rupture
NRC	Noise Reduction Coefficient
OPC	Ordinary Portland Cement
SRI	Sound Reduction Index
UBBL	Uniform Building By-Laws

## CHAPTER 1

### INTRODUCTION

#### 1.1 General Introduction

Concrete is commonly utilised in the construction industry regardless of its density. For instance, normal-weight or high-strength grade concrete is frequently utilised in load-bearing structural elements; lightweight concrete is often used for non-load-bearing elements such as wall panels. Precast technology is an advanced construction method, producing building elements with proper supervision off-site and assembling them on-site. Using recycled materials in construction can fulfil the Green Building Index (GBI) criteria where the green building concept has gained popularity, and precast technology can play a significant role in its development. Further research on utilising recycled materials in precast concrete production can also contribute to more sustainable development in the construction industry.

The global tyre manufacturing industry involves approximately 160 primary manufacturers across 45 countries, leading to waste tyre management becoming a significant environmental issue worldwide (De Maeijer et al., 2021). According to Nor and Ishak (2016), around 8.2 million waste tyres are generated annually in Malaysia. Recycling and reusing waste tyres is an alternative solution to tackle this problem. Grinding waste tyres can produce rubber aggregate or rubber particles that can substitute mineral aggregate in concrete to produce either rubberized concrete or rubberized lightweight foamed concrete. Incorporating recycled rubber particles in a concrete mixture can reduce waste tyre disposal's environmental impact and decrease the overconsumption of mineral aggregates such as stone and sand (Eltayeb et al., 2022). The coarse aggregate is omitted to produce lightweight wall panels, and a foaming agent is added to reduce the density of the concrete mixture. Fine aggregate is then replaced with powdered crumb rubber, with the replacement proportion adjusted according to the desired strength for different applications.

Numerous studies on rubberized concrete have proved its excellent properties, including improved dynamic properties, higher energy absorption capacity, better ductility, enhanced abrasion and impact resistance, as well as good sound insulation, compared to standard or plain concrete. However, replacing the aggregate with rubber particles can result in drawbacks, such as reduced compressive and tensile strength, which are significant factors in load-bearing structures. Nonetheless, the current study's load-bearing capacity of rubberized concrete is not a concern since the focus is on the non-load-bearing wall panel made of rubberized lightweight foamed concrete.

The first patent introduced the rubber crumb-reinforced cement concrete was by a pioneer named Frankowski in 1992 (De Maeijer et al., 2021). However, it is essential to note that there may be a lack of research specifically on rubberized lightweight foamed concrete. On the other hand, numerous studies have examined the properties as well as the performance of both foamed and rubberized concrete. Therefore, in this study, multiple product and laboratory tests are done to expand the knowledge and understanding of the sound transmission behaviour, fire-resisting properties, and structural performance of the full-scale rubberized lightweight foamed concrete with the skin layers of magnesium oxide board.

## **1.2 Importance of the Study**

The sandwiched wall panel system can be an alternative to the conventional brick wall system. Utilising a lightweight sandwiched wall panel system can minimise the construction time and cost as precast wall panels are produced within a controlled environment and transported to the construction site for installation. The precast wall panel installation can be completed faster than the conventional brick wall system, requiring longer construction time for bricklaying and mortar curing.

In addition, the reduced load will minimise the beam's internal forces, resulting in a smaller beam size. At the same time, the load transferred to the column can be reduced, and the column's size can also be optimised. As a result, overall construction costs can be more economical since less load applied may result in a lower load-bearing capacity required for a foundation. Furthermore, precast wall panels produced with a core of rubberized lightweight foamed



concrete can reduce the overall sizing and reinforcement of the structural member and further reduce the construction cost since the usage of concrete volume and steel tonnage is minimised. Moreover, the time for concrete casting and steel bar erecting will be kept to a minimum level.

Cement is the main material used to produce concrete, but the cement industry has contributed to 5 % of the total carbon dioxide emissions worldwide (Hasanbeigi, Price and Lin., 2012). In addition, extra carbon dioxide emissions will result from steel production. Thus, reducing concrete and steel in construction will eventually lower the carbon dioxide emission rate. Furthermore, utilising sustainable materials such as rubberized lightweight foamed concrete can reduce carbon emissions, promotes a more sustainable construction industry, and push Malaysia to a carbon-neutral nation.

On the other hand, this study can evaluate the sound absorption, fire resistance rating, and flexural strength of the sandwiched wall panel consisting of rubberized lightweight foamed concrete with a magnesium oxide board as the skin layers. These properties are crucial for commercialising the sandwiched wall panel. Once the properties are determined, the crumb rubber can be incorporated into the wall panel system in building construction. As a result, the global issue of waste tyre management can be addressed, and the environmental pollution from waste tyres disposal can be prevented. Furthermore, this innovative approach can extend the life cycle of rubber tyres. The Industrialised Building System (IBS) construction technology can be more appealing as the investigated sandwiched wall panel can be mass-produced as precast panels.

### 1.3 Problem Statement

The waste material production rate is rising dramatically at an alarming speed worldwide (Kashani et al., 2017). Waste rubber output worldwide is up to 20 million tonnes annually, ranked second place in waste polymer materials. The development of the economy and urban transportation results in a massive waste of rubber tyres attributed to the inclining of car quantities (Jin, Yin and Yu, 2022). The generated scrap tyre is estimated to reach a new high level, 1.2 billion tonnes annually, by 2030 (Lim et al., 2020). In Malaysia, 8.2 million waste tyres, equivalent to 57 391 tonnes of waste tyres, reach their life cycle stage of end-of-life annually (Nor and Ishak, 2016). Thus, an effective way to extend the life cycle of waste tyres is essential to cope with the increasing utilisation of rubber tyres.

According to Nor and Ishak (2016), handling and managing waste tyres is challenging since waste tyres are not readily biodegradable compared with other organic materials. Thus, there are more sustainable ways to handle waste tyres than landfilling. According to Zhang and Poon (2018), landfilling will potentially cause the leakage of contaminants and pollute the environment. The pollutants include the by-product of waste tyres reacting chemically with methane gases. In short, Wang et al. (2019) stated that waste rubber is difficult to be decomposed under natural condition and bring pollution to the environment. The researcher also found that waste tyre disposal will get a lot of negative impacts, such as the potential fire hazards and the breeding of mosquitoes which will be the hotbed for infectious diseases.

Apart from landfilling, the other conventional disposal approach is incinerating. However, the toxic gases emitted from the combustion of waste tyres will threaten the living organisms surrounding them. Moreover, the current disposal methods of waste tyres are not a suite and friendly *modus operandi* for the environment. Thus, innovatively using waste tyres can save resources and prevent environmental pollution (Wang et al., 2019).

#### **1.4 Aim and Objectives**

This study aims to produce and evaluate the engineering properties of a sandwiched wall panel made of rubberized lightweight foamed concrete with a fresh density of  $1150 \text{ kg/m}^3$  as a core layer and magnesium oxide board as the skin layers. The objectives of this project are:

- (i) To study the sound absorption for the full-scale rubberized lightweight foamed concrete with magnesium oxide board as the skin layers.
- (ii) To investigate the fire resistance rating of 120 minutes for the full-scale rubberized lightweight foamed concrete with the magnesium oxide board as the skin layers.
- (iii) To evaluate the flexural strength of the full-scale rubberized lightweight foamed concrete with the magnesium oxide board as the skin layers.

### 1.5 Scope and Limitation of the Study

This study mainly focuses on the engineering properties of sound absorption, fire-resisting properties, and flexural strength of rubberized lightweight foamed concrete with the skin layers of magnesium oxide board. Powdered crumb rubber is utilised in this study with an 80 % replacement proportion. Furthermore, the water-cement ratio is fixed at 0.55 to produce the rubberized lightweight foamed concrete within the density of  $1150 \text{ kg/m}^3$ . Finally, a foaming agent is added to the fresh concrete mixture to achieve the targeted density.

The rubberized lightweight foamed concrete specimen is cast at  $600 \text{ mm} \times 600 \text{ mm} \times 80 \text{ mm}$  for all the product and laboratory tests. In addition, a 9 mm thick magnesium oxide board is used for the skin layers to fabricate the sandwiched wall panel. The TPS Thin Bed Adhesive Premium 668 provides adhesiveness between the rubberized lightweight foamed concrete and the magnesium oxide board. The thickness of the TPS is applied at 3.5 mm to 4 mm on each side. Thus, the fabricated sandwiched wall panel thickness will be around 105 mm.

The area required for the sound transmission behaviour is  $10 \text{ m}^2$  for the standard testing requirements. Thus, twenty-eight specimens are used in the sound transmission behaviour. For the fire-resisting properties, the area required is  $9 \text{ m}^2$  for the standard testing requirements. One specimen is sufficient for the structural performance testing to do the flexural test. All the rubberized lightweight foamed concrete specimens have water curing for 28 days.

The limitation of this study is that the sound transmission behaviour is only focused on the Sound Reduction Index (SRI) of the wall panel at different third-octave frequencies instead of sound reflection. Furthermore, the fire-resisting properties are only focused on the ability of the wall panel to sustain a 120-minute fire resistance rating as well as a 90-second hose stream test. Besides, the flexural strength of the wall panel is tested at  $600 \text{ mm} \times 600 \text{ mm}$ , and the flexural test can only find the maximum load applied on the midspan of the wall panel until the wall panel is cracked.

## **1.6 Contribution of the Study**

This study investigates the engineering properties of rubberized lightweight foamed concrete with the skin layers of magnesium oxide board as a sandwiched wall panel system. The sound absorption, fire resistance rating, and flexural strength determined can contribute to market commercialization. These properties are essential to meet the standard requirement for commercializing the sandwiched wall panel in building construction. As a result, this study will eventually contribute to developing more sustainable building materials and construction practices.

Furthermore, incorporating crumb rubber into the rubberized lightweight foamed concrete presents an executable solution to the global issue of waste tyre management. This innovative method in the construction industry can mitigate the environmental impact of waste tyre disposal and provide an extendable life cycle for rubber tyres. This approach can also contribute to waste materials reusing and recycling, promoting sustainability in the construction industry.

In addition, the precast sandwiched wall panel can also contribute to the development of the Industrialised Building System (IBS) since the sandwiched wall panel can be produced with mass production in a factory with high standards from raw materials selection to transportation to the construction site. As a result, the precast sandwiched wall panel can offer a shorter construction time and high-quality outcome, which is more attractive than the conventional brick wall system. Thus, this study can contribute to the IBS development and boost the construction industry's transformation to achieve a more sustainable future.

## **1.7 Outline of the Report**

This report consists of five chapters to provide a comprehensive study regarding the incorporation of crumb rubber in rubberized lightweight foamed concrete for its engineering properties.

Chapter 1 illustrates the overview, including the introduction, the study's importance, and the study's contribution. Besides, the problem statement, aim and objectives, as well as scope and limitations, are also clearly stated. Finally, this chapter ended with the outline of the report for the information organisation.

Chapter 2 discusses the literature view for a better understanding of the study. The topics reviewed include types of lightweight concrete and rubberized lightweight foamed concrete. Moreover, the types of rubber aggregate and the application of crumb rubber are covered. Finally, the fresh and hardened properties of rubberized lightweight foamed concrete are discussed, followed by the introduction to the sandwiched wall panel and the magnesium oxide board.

Chapter 3 describes the raw materials as well as methods applied in this study. In the methodology section, the information included is the raw materials preparation, concrete mixing, concrete casting, and concrete curing. The steps of skin layer installation are also clearly stated, followed by the four product and laboratory tests procedure: acoustic insulation test, fire resistance rating test, hose stream test, and flexural strength test.

Chapter 4 presents the test results and a discussion of the outcomes obtained. The qualitative observation and quantitative measurement are recorded and tabulated in tables and graphs for a better presentation to illustrate the engineering properties of the sandwiched wall panel, including the Sound Reduction Index (SRI), fire resistance rating, and the Modulus of Rupture (MOR).

Chapter 5 summarises the results obtained from the product and laboratory tests according to the objectives stated. Finally, the conclusion and future research recommendations are discussed to conclude the information obtained during the study.

## CHAPTER 2

### LITERATURE REVIEW

#### 2.1 Introduction

The literature review provides an overview of types of lightweight concretes, types of rubber aggregates, and the application of crumb rubber in concrete. In addition, the engineering properties of the rubberized lightweight foamed concrete are reviewed to explore the current research on it. Furthermore, the introduction to the sandwiched wall panel and magnesium oxide board is presented in this review. This literature review is a foundation platform for this study to demonstrate the need to develop an innovative and sustainable approach to mitigate waste tyre management issues. Overall, the literature review aims to illustrate the potential of rubberized lightweight foamed concrete as a construction material to contribute to sustainable construction industry development.

#### 2.2 Types of Lightweight Concrete

Lightweight concrete is not a modern innovation but a new achievement in developing concrete technology. It has been well-known since the start of the Roman Empire, whereby that lightweight concrete was built two thousand years ago, and the best example is the Pantheon in Rome (Thienel, Haller and Beuntner, 2020). There are numerous approaches to lightweight concrete preparation by utilising different types of material. Thus, lightweight concrete can be further classified as well as divided into four different types which are:

- (i) Lightweight Aggregate Concrete
- (ii) No Fines Concrete
- (iii) Aerated Concrete
- (iv) Lightweight Foamed Concrete.

##### 2.2.1 Lightweight Aggregate Concrete

During ancient times, lightweight aggregate concrete originated from the natural pumice stone and other types of porous rocks with volcanic origin (Szydlowski and Mieszcak, 2017). Nowadays, lightweight aggregate is porous and low in

specific gravity, and it can be found in either natural or artificial sources. For the natural aggregate, the aggregates are from volcanic origin. For the artificial aggregate, the aggregates are extracted from expanded blast-furnace slag, vermiculite, and clinker aggregate (Ismail, Fathi and Manaf., 1997).

Furthermore, lightweight aggregate concrete is divided into two categories based on its usage and application. The two types are lightweight aggregate concrete with partial compaction and structural lightweight aggregate concrete. The main properties of the partially compacted lightweight aggregate concrete are low density and adequate strength to gain good thermal insulation and low drying shrinkage to prevent cracking. On the other hand, structural lightweight aggregate concrete has full compaction as dense aggregate in regular concrete. Therefore, it can be utilised with steel reinforcement to provide good bonding and adhesiveness between the steel and concrete. In addition, the concrete is also acted as a protective layer for the steel from getting corrosion (Ismail, Fathi and Manaf., 1997).

### **2.2.2 No Fines Concrete**

No-fines concrete is denoted as porous concrete, whereby the omitting of fine aggregate in concrete mix design is done. The density of no-fines concrete has a lower density and capacity of strength due to its porous microstructure. Furthermore, the no-fines concrete's water-cement ratio will affect the concrete mixture's porosity and workability. A high water-cement ratio will reduce the density since the free water in contact with no-fines concrete that penetrated and occupied the space within the concrete mixture will eventually evaporate and dry up after the curing process. On the other hand, a low water-cement ratio will cause the cement paste to be dry, and the bonding between the cement paste and coarse aggregate will be insufficient (Jiahao et al., 2019). Generally, the usage and application of the no-fines concrete are road pavement and surface treatment for water draining. However, no-fines concrete can also be used for non-structural applications, including reinforced panels, due to its suitable properties in acoustic, thermal, and permeability (Carsana, Tittarelli and Bertolini., 2013).



### **2.2.3 Aerated Concrete**

Aerated concrete is more homogeneous than regular concrete since the coarse aggregate is absent in aerated concrete. The materials used for the aerated concrete are cement, fine aggregate, water, and other additive chemicals. Aerated concrete is lightweight, with air voids entrapped inside the mortar matrix using a suitable aerating agent. Aerated concrete is another type of cellular concrete with the advantage of being lightweight, which will eventually become more economical when constructing structural elements such as foundations. In addition, aerated concrete can have a higher degree of thermal insulation and save material consumption during production due to its porous properties (Narayanan and Ramamurthy, 2000).

### **2.2.4 Lightweight Foamed Concrete**

Lightweight foamed concrete is a homogeneous pore structure consisting of a cement filler matrix or denoted as mortar. The porous structure is created by introducing air into the mixture, and the air is in the form of tiny bubbles (Othuman and Wang, 2011). A foaming agent is used in lightweight foamed concrete. It is a chemical that creates tiny air bubbles and is enclosed by reducing the tension on the surface of the form solution and increasing the air bubbles' stability (Panesar, 2013).

Lightweight foamed concrete consists of ample attractive advantage properties including excellent thermal as well as acoustic insulation, well self-flowing, and simple procedure for fabrication. Each air pore will contribute to heat conduction at a relatively low level of temperature (Othuman and Wang, 2011). At a high-temperature level, radiation will significantly affect the thermal conductivity since the pore structure due to the air will eventually cause the radiation. The well thermal and acoustic performance shows the possibility for market commercialisation of lightweight foamed concrete as building materials (Othuman and Wang, 2011).

The mechanical properties, such as the compressive and flexural strength of lightweight foamed concrete, are relatively low compared to normal-strength concrete. However, it still can be utilised as a wall partition or light load-bearing wall for the building.

### **2.3 Rubberized Lightweight Foamed Concrete**

Rubberized lightweight foamed concrete is categorised as lightweight foamed concrete without adding coarse aggregate and partially replacing the fine aggregate with crumb rubber. When comparing conventional concrete with rubberized concrete, a lower value in density is exhibited in the rubberized concrete (Pham et al., 2020). The lightweight foamed concrete will show a lower density value than conventional concrete.

Crumb rubber concrete has an excellent performance in several properties, such as high resistance towards cracking and shrinkage, good heat insulation, high toughness, and low modulus of elasticity (Wang et al., 2019). Besides, the compressive strength is relatively weak and low compared with normal concrete (Wang et al., 2019). According to Wang et al. (2019), a smaller particle size of crumb rubber will further decrease the compressive strength of the rubberized lightweight foamed concrete. However, it will have a significant improvement in thermal insulation. Furthermore, the capacity of the rubberized lightweight foamed concrete in the ability of energy absorption against the impacted load will be improved (Pham et al., 2020). The increasing particle friction between the two primary materials, cementitious matrix and crumb rubber particles, contributed to the greater capacity for energy absorption (Pham et al., 2020).

Besides, adding the crumb rubber into the concrete mixture will also eventually affect the interfacial transition zone (ITZ) between the rubber particles and the cement paste (Wang et al., 2012). The broader width of the ITZ between the rubber paste and shale ceramsite-paste is found when more crumb rubber is added (Wang et al., 2012). Thus, the flexibility of the rubberized lightweight foamed concrete can be improved by making the dosage adjustment for the crumb rubber. Eventually, the microhardness of the concrete can also be controlled (Wang et al., 2012).

## **2.4 Types of Rubber Aggregates**

Rubber aggregates can replace coarse and fine aggregates in the concrete mixture. Different shapes and sizes of the rubber aggregate will be categorised into different groups. The divided categories are chipped rubber, crumb rubber, and ash rubber (Fiore et al., 2014).

### **2.4.1 Chipped Rubber**

Chipped rubber ranging from 25 mm to 30 mm will replace the coarse aggregate in the concrete mixture (Fiore et al., 2014). Chipped rubber is also known as shredded rubber. The study found that replacing the normal coarse aggregate with chipped rubber will eventually cause a decrease in compressive strength, split tensile strength, as well as flexural strength (Parhi, 2015). The main factor in the reduction in strength is the poor bonding between the rubber particles and the cement paste. In addition, the large size of the chipper rubber causes uneven distribution during the mixing process since it cannot fit into the interfaces within the concrete mixture and the aggregates available (Zheng, Huo and Yuan, 2008).

### **2.4.2 Crumb Rubber**

Crushing automobile waste tyres can produce crumb rubber (Wang et al., 2019). Parhi (2015) states that crumb rubber can be produced through various mechanical processes. The processes are granulation, followed by the cracker milling process, and ended with magnetic separation. Both granulation and cracker milling will cut the waste rubber into smaller particles according to the specific requirement. Meanwhile, magnetic separation will eventually remove the inorganic materials in the waste rubber mixture, such as the magnetic steel fabric wire. Therefore, crumb rubber ranging from 3 mm to 10 mm will replace the fine aggregate in the concrete mixture (Fiore et al., 2014). Parhi (2015) stated that the size of the crumb rubber would range from 0.425 mm to 4.75 mm between the chipped rubber and ground rubber. In short, crumb rubber is a type of rubber that can be obtained easily in the market. Thus, it has been selected to be utilised in the study to replace the normal fine aggregates in the concrete mixture partially.

### **2.4.3 Ground Rubber**

Parhi (2015) states that ground rubber particles are the smallest size among the three rubber aggregates. Ground rubber, denoted as ash rubber, is smaller than 1 mm, which will act as the filler in the concrete mixture (Fiore et al., 2014). The production of ground rubber passes through two stages which are magnetic separation as well as a screening process. Ground rubber can be used as a replacement for cement with a specific ratio. The cement content replacement can be done using ground rubber through micro-milling (Sofi, 2018). The small size of ground rubber is suited for partial cement replacement. However, it will reduce the overall concrete workability due to the low friction between rubber particles and cementitious materials (Thomas, Gupta and Panicker, 2015). With the increase in ground rubber replacement of cement in the concrete mixture, the concrete mixture will show higher flexural strength than the concrete mixture with the chipped rubber replacement (Ganjian, Khorami and Maghsoudi, 2009).

### **2.5 Application of Crumb Rubber**

Currently, crumb rubber is utilised in the asphalt pavement industry (Zhu and Carlson, 1999). According to the authors, the ultimate product formed after adding the crumb rubber is named crumb rubber modified asphalt (CRMA). This product can be used in road construction, highway construction, building, or other public facilities such as car parking lots. In addition, the garden hoses, floor mats, horse trails, playground chips, and some roofing materials utilise crumb rubber as the raw materials. However, due to the high cost, the utilisation rate of the crumb rubber from waste tyres still needs to be higher.

Zhu and Carlson (1999) proposed utilising crumb rubber in highway noise barriers. According to the author, traffic noise is caused by a few situations, such as friction between the body of vehicles and the air touching the surface of vehicles and the tyres contact with the road pavement. The traffic noise falls between the frequency easily detected and heard by humans, ranging from 250 Hz to 4000 Hz. Plain concrete is relatively weak in sound absorption, and thus crumb rubber is added to the concrete to increase the effectiveness of sound absorption.

Furthermore, crumb rubber can be the shock-wave absorber when an earthquake occurs. According to Chiaro et al. (2019), adding crumb rubber into the concrete mixture will eventually reduce the acceleration due to seismic by 27 %. Besides, the properties of the concrete will change from brittle to ductile after the crumb rubber is added to the concrete mixture (Chiaro et al., 2019).

In a nutshell, crumb rubber is mainly used for road construction, pavement, and noise barrier. Crumb rubber absorbs the shock wave of building structures due to the earthquake. This study will focus on applying the crumb rubber for the sound transmission behaviour for the rubberized lightweight foamed concrete sandwiched wall panel.

## **2.6 Fresh Properties of Rubberized Lightweight Foamed Concrete**

### **2.6.1 Workability**

Workability can allow the concrete mixture to be poured and cast in any shape as required (Fawzy, Mustafa and Elshazly, 2020). Workability can also be denoted as a concrete mixture's mixing, handling, and compaction. According to Fawzy, Mustafa and Elshazly (2020), increasing the rubber grade will eventually reduce the workability of rubberized concrete due to large particles will reduce the concrete flowability. The workability of the concrete mixture will decline significantly when the rubber particles reach the replacement percentage up to 30 % and above (Fiore et al., 2014). Fiore et al. (2014) also stated that the higher viscosity of concrete mixture with rubber particles caused a remarkable drop in workability.

On the other hand, Fawzy, Mustafa and Elshazly (2020) also stated that the slump value will decrease with the reduction of rubber grain size. The surface of rubber particles is spiky, a crucial factor in slump reduction (Bing and Ning, 2014). However, the slump value improvement will be noticeable when chipped rubber is utilised in the coarse or fine aggregate replacement of the concrete mixture.

According to Eltayeb et al. (2020), the fluidity test was conducted according to the standard slump cone test without compaction or applying the rodding for the fresh concrete mix. The outcome obtained from the author is the diameter of concrete slump flow will decrease by 5 %, 4.7 %, and 5.5 % for the water-cement ratio of 0.5 and rubber content replacement by 10 %, 20 %, and

30 %, respectively. Another set of data is obtained, the results are the diameter of concrete slump flow will decrease by 5 %, 4.7 %, and 5.5 % for the water-cement ratio of 0.38 and rubber content replacement by 4.2 %, 6.7 %, and 11.7 %, respectively. Concluding the slump cone test done by the author, the inclining replacement proportion of rubber content will reduce the fluidity or workability of the concrete mixture, and the lower water-cement ratio will also decrease the workability of the concrete mixture. The results obtained by this author are similar to Fiore et al. (2014), whereby the remarkable workability will be evident when the rubber content replacement proportion is up to 30 %.

In conclusion, a large amount of crumb rubber is not conducive when pouring rubberized lightweight foamed concrete. Thus, the content of crumb rubber should be measured and controlled at 3 % (Wang et al., 2019). According to Wang et al. (2019), the controlled value of 3 % crumb rubber content can ensure the control of the increasing friction between the bubbles and the thickening of the slurry. Furthermore, this can ensure the workability of the rubberized lightweight foamed concrete is within the acceptable range whereby the fluidity is measured as 180 mm, which is done by Wang et al. (2019).

## **2.7 Hardened Properties of Rubberized Lightweight Foamed Concrete**

### **2.7.1 Density**

Rubberized concrete has a 2 % to 11 % lower weight than ordinary concrete (Elshazly, Mustafa and Fawzy., 2020). The addition of rubber particles into the concrete mixture will reduce the dry unit weight and directly reduce the density of the concrete mixture (Bing and Ning, 2014). Rubber particles possess lower density than conventional coarse and fine aggregate in the concrete mixture. However, Bing and Ning (2014) stated that the amplitude of unit weight and density reduction could not be justified by calculating the density difference of the materials used, which are the rubber particles and the coarse and fine aggregate. The main reason is that the rubber particles have varied air content based on size. The rubber particles with angular shapes will create large air voids, leading to high porosity within the concrete mixture (Ling, 2011). Moreover, Ling (2011) stated that rubber particles tend to have air entrapment

from surroundings caused by their unique behaviour, which is non-polarity and further decreases the density of the concrete mixture with rubber particles.

According to Eltayeb et al. (2020), the lower density of rubber particles compared with fine aggregate is the main reason for the lower density of the concrete produced. The statement is similar to Bing and Ning (2014), supported by the experiment by Eltayeb et al. (2020). In the experiment, the rubber content replaces the fine aggregate at a different proportion. The ultimate results show a density reduction of 4.1 %, 6.7 %, and 9.1 % for 10 %, 20 %, and 30 % replacement, respectively.

According to Ling (2011), increasing the water-cement ratio increases the concrete density when the rubber content is fixed in a concrete mixture. The author mentioned that the presence of water would fill up the space or so-called structure pores and thus increasing the concrete density. Furthermore, Eltayeb et al. (2020) also proved that the water-cement ratio would proportionally affect the density. In the experiment done by the author, the reduction of the water-cement ratio from 0.5 to 0.38 will eventually reduce the foam concrete density by 5.2 %. In short, the density of the rubberized concrete will be lower than the plain concrete. At the same time, the density of the rubberized lightweight foamed concrete will be even lower since the foam is utilised in the mixture, and the coarse aggregate is also omitted. On the other hand, rubberized concrete with lower water content will have a lower density. This property is also applied to the rubberized lightweight foamed concrete due to its similarity to the aggregate replacement by rubber particles.

### **2.7.2 Compressive Strength**

Rubber particles can be used to replace both fine and coarse aggregate. According to Fawzy, Mustafa and Elshazly (2020), the compressive strength of the concrete will reduce by 85 % when the coarse aggregate replaces the rubber particles. On the other hand, the compressive strength of the concrete will decrease by 65 % when the rubber particles replace the fine aggregate. From the other side study done by Fawzy, Mustafa and Elshazly (2020), the loss of compressive strength for the concrete mixture will be up to 50 % for both coarse and fine aggregate replacement, depending on the replacement proportion of the rubber particles. The critical strength reduction factor is the air voids within the concrete mixture. The number of air voids will increase with the number of rubber particles. Thus, the compressive strength will decrease when the rubber content rises. However, declining strength can be minimised by adding the de-airing material into the concrete mixture.

Fawzi et al. (2020) also outlined the factor contributing to compressive strength loss. Lacking bonding between the cement paste and the rubber particles will cause the soft cement paste that binds the rubber particles to crack when the load is applied to the concrete. NaOH solution can be used in the rubber treatment to increase the bond strength between rubber and cement. However, when the replacement of rubber content increases, the compressive strength of the concrete will show a tendency to decrease (Ling, 2011). Ling (2011) stated that 70 % of compressive strength is reduced in the concrete with 50 % rubber content, decreasing from plain concrete of 42.5 MPa to 12.4 MPa. The author also stated that replacing the rubber content would increase the volume for the weakest phase and the interfacial zone.



### 2.7.3 Flexural Strength

Flexural strength is defined as the capability of a material to withstand the bending forces exerted perpendicular to its longitudinal axis. When the rubber particles are used to replace 20 % of the fine aggregate, the flexural strength of the concrete will decrease by 12.8 %. However, when the rubber particle size is reduced, the loss of flexural strength will also be reduced. On the other hand, a reduction in the flexural strength will be more evident in the coarse aggregate instead of fine aggregate for the rubber particles replacement. However, the rubberized concrete's flexural stiffness is enhanced when the water-to-cement ratio decreases. Adding silica fume will also emphasise the flexural stiffness due to the bond enhancement realized (Fawzy, Mustafa and Elshazly, 2020).

According to Eltayeb et al. (2020), the flexural strength of the concrete specimen will increase with the replacement proportion of rubber content. The final results obtained from the increase in flexural strength test are 9.5 %, 13.3 %, and 1.3 % for the replacement portion, with 8.47 %, 17 %, and 47.8 %, respectively. The rate of flexural strength increase keeps on inclining to replace rubber content of less than 17 %. When the replacement portion exceeds 17 %, the increasing rate of the flexural strength test decreases, meaning that the replacement portion of 17 % for rubber content will contribute to the strongest flexural strength. Eltayeb et al. (2020) mentioned that the reduction in foam volume is the main contributor to flexural strength enhancement.

#### 2.7.4 Fire Performance

Fire resistance at a high-temperature stage for rubberized lightweight foamed concrete will show a remarkable improvement due to its unique property, which is a porous structure (Sayadi et al., 2016). According to the author, the heat transfer for a porous structure will be affected by radiation. Radiation is defined as the inverse function of the number of air-solid interfaces.

Lightweight foamed concrete (LFC) can be used as a fire-resisting material for a partition or a load-bearing wall in low-rise construction (Othuman and Wang, 2011). Based on the experiment set up by the author, the fire resistance requirement is deduced based on the thermal insulation of the wall. The relevant standard is taken from EN 1991-1-2, whereby the thermal boundary condition is followed by the code mentioned. In short, the experiment ensured the average temperature of the unexposed surface did not exceed the level of 140 °C. Table 2.1 shows the results obtained from the author regarding minimum thickness for the lightweight foamed concrete for different fire resistance ratings, including 30 minutes, 60 minutes, 90 minutes, and 120 minutes. The density for LFC density used is 650 kg/m<sup>3</sup> and 1000 kg/m<sup>3</sup>.

Table 2.1: Minimum LFC Thickness for a Different Level of Fire Resistance Rating (Othuman and Wang, 2011).

LFC density (kg/m <sup>3</sup> )	Minimum LFC thickness (mm) for fire resistance rating of			
	30 minutes	60 minutes	90 minutes	120 minutes
650	21.0	36.7	50.1	60.5
1000	23.1	39.1	52.3	63.2

Besides, Pereira et al. (2016) stated that fire performance characteristics for a sandwiched wall panel are the integrity as well as the thermal insulation. According to Pereira et al. (2016), integrity is defined as the ability of the fabricated sandwiched wall panel to withstand fire exposure at one side, without transmitting fire to the unexposed side of the wall. In addition, Pereira et al. (2016) also mentioned that thermal insulation is denoted as the capability of the sandwiched wall panel to withstand fire exposure at one side, without transmitting significant heat to the unexposed side.

### 2.7.5 Thermal Properties

The evaporation of water molecules will occur at high temperatures (Fawzy, Mustafa and Elshazly, 2020). According to Fawzy, Mustafa and Elshazly (2020), the water molecules evaporated are from the molecule, which is bonded chemically, and moved freely within the capillary pores inside the concrete mixture and within the water molecules inside Calcium Silicate Hydrate (C-S-H) gel and sulphoaluminate.

When the temperatures reach 300 °C, the water evaporation will eventually cause the concrete to shrink. C-S-H gel will be decomposed after the temperature is above 400 °C. When the temperature is reached, the transformation of calcium hydroxide to anhydrite lime will occur (Fawzy, Mustafa and Elshazly, 2020). The high temperature will cause the concrete to be cracked, and the compressive strength will reduce and be lost due to the cracking. The main reason is that the rubber inside the concrete will burn up with the temperature. Thus, when the addition of rubber content increases, the loss of compressive strength in the concrete mixture will be even faster due to more pores being left within the concrete structure.

Thermal conductivity ( $k$ ) is happening under a steady state condition. It is the quantity measurement for the heat transmission in the normal direction to the unit area surface due to temperature gradient (Sukontasukkul, 2009). Therefore, the thermal conductivity is always inversely proportional to the density. Thus, the rubberized lightweight foamed concrete with lower density is expected to have lower thermal conductivity than the typical concrete mixture.

Furthermore, Sukontasukkul (2009) also stated that crumb rubber concrete exhibited lower performance in heat transfer and thus had higher heat resistivity than plain concrete. The size of the crumb rubber particles and the rubber content will affect the heat transfer rate, whereby larger and more crumb rubber particle content will increase the rate for transferring the heat.

### 2.7.6 Acoustics Properties

Rubberized concrete is suitable for absorbing the sound passing through it and the shaking energy (Fawzy, Mustafa, and Elshazly, 2020). Therefore, the ultrasonic modulus will reduce with the increased content and the rubber concentration applied. This results from the nature of the rubberized concrete, a porous structure that will be magnified with the increasing rubber content (Fawzy, Mustafa, and Elshazly, 2020).

The study by Zhang and Poon (2018) concluded that rubberized concrete with a high proportion of recycled rubber aggregate replacement would significantly enhance sound insulation properties. Besides, the study also concluded that using rubber aggregate with pre-treatment will improve the sound insulation of the rubberized concrete (Zhang and Poon, 2018). Zhang and Poon (2018) also stated that the rubberized concrete would perform well in insulating the sound compared with the concrete mixture without the incorporation of crumb rubber.

The sound absorption coefficient ( $\alpha$ ) can be utilised as the parameter to measure the ability of a material to have sound absorption (Sukontasukkul, 2009). In the experiment by Sukontasukkul (2009), two different frequency ranges are selected: low-mid frequency and high frequency. The frequencies used in the low-mid range are 125 Hz, 250 Hz, and 500; the frequencies used for the high range are 1000 Hz, 2000 Hz, and 4000 Hz. According to Sukontasukkul's (2009) results, concrete with crumb rubber incorporation has started to show significantly better sound absorption ability at the high-frequency ranges or above 1000 Hz compared with plain concrete.

Due to the complexity of indicating the sound absorption coefficient at a different frequency, the author utilises a parameter named noise reduction coefficient (NRC). The NRC will be obtained using the sound absorption coefficient from different frequencies, including 250 Hz, 500 Hz, 1000 Hz, and 2000 Hz. The summation of the coefficients obtained and divided by four will eventually determine the noise reduction coefficient of the concrete with and without crumb rubber. According to the results obtained by the author, plain concrete recorded the lowest NRC, which is 12.94 %, and the concrete with 10 % crumb rubber will have a lower NRC value compared with the concrete with 20 % crumb rubber. Table 2.2 shows the noise reduction coefficient for each

type of concrete with different percentages of crumb rubber and different types of crumb rubber of No. 6 and No. 26. In short, the concrete with 20 % crumb rubber from the combination of No 6. Crumb rubber recorded the highest value, with 18.94 %.

Table 2.2: Noise Reduction Coefficient for a Different Type of Concrete with Different Crumb Rubber Content (Sukontasukkul, 2009).

<b>Concrete Type</b>	<b>Noise Reduction Coefficient (%)</b>
<b>PC</b>	12.94
<b>6CR10</b>	18.12
<b>6CR20</b>	18.19
<b>26CR10</b>	15.88
<b>26CR20</b>	18.25
<b>626CR10</b>	6.25
<b>626CR20</b>	18.94

Maurin and Kwapisz (2021) found that noticeable differences and discrepancies in the low-frequency range between 50 Hz to 80 Hz attributed to uncertainties in the measurement. To address this issue, the authors suggest using more octave band frequencies when examining a similar specimen, which can help minimize the variation obtained within the low-frequency range since more modes are present in the octave band. On the other hand, the authors also mentioned that the results obtained from the frequencies ranging from 3200 to 5000 Hz will experience significant differences. The main reasons are the measurements do take the loss factor effect as well as the indirect transmissions into consideration.

## 2.8 Sandwiched Wall Panel

Precast concrete sandwich wall panels are popular in market utilisation for the construction industry due to their excellent thermal as well as structural performance (Kumar et al., 2021). Kumar et al. (2021) stated that sandwiched wall panels had become the ultimate choice for those who intend to reduce the consumption of energy as well as pay attention to global warming issues. Energy consumed to heat up and cool down the interior building space will decrease significantly after utilising the sandwiched wall panels due to their thermal insulation ability.

Sandwich structures are composite structures with a core material with low-density properties and two thin and stiff faces (Bharath et al., 2022). Furthermore, the overall thickness of composite sandwiched wall panels will decrease as much as two third compared with the non-composite wall panel. As a result, the self-weight reduction of the wall panels can be achieved, and the performance of sandwiched wall panels towards the seismic resistance will also improve. According to Kumar et al. (2021), the crushing failure is mainly due to three vital parameters: the thickness of provided insulator, the spacing between the connector installed, and the slenderness ratio. According to Bharath et al. (2022), the flexural rigidity of the sandwich structure relies not only on material properties such as Young's Modulus but also on the increase of the inertia.

Time lag and the decrement factor are crucial characteristics of materials on the heat storage capacity (Ng, Low and Tioh, 2011). According to the author's studies, occupants in an enclosed indoor space will enjoy the comfortable indoor temperature even if the temperature outside the space is at a very high level or in fluctuating circumstances. Generally, a material possesses a long-time lag, with eventually causes a low level in the decrement factor. The time lag is denoted by the time taken for a heat wave to be propagated from the outer surface to the inner surface. In contrast, the decrement factor is denoted by the decreasing ratio of the heat wave amplitude during the propagation throughout the wall panel (Ng, Low and Tioh, 2011).

## **2.9 Magnesium Oxide Board**

Magnesium Oxide (MgO) has good performance in various properties such as acoustic properties, resistance to the impact applied, structural strength, and survivability during its working life (Rusthi et al., 2017). The author has also discussed the chemical composition of the magnesium oxide board. According to Rusthi et al. (2017), the main constituents of the magnesium board consist of two, which are Magnesium Oxide (MgO) and Magnesium Chloride (MgCl<sub>2</sub>). The other minor components are added to the magnesium oxide board to improve and enhance the properties. The improvements included better insulation against sound and heat. The minor constituents are Perlite, Woodchip, and Fiberglass.

Magnesium oxide board is a material that can resist high temperatures up to 800 °C (Mokrenko and Kozlovská, 2020). Besides, Mokrenko and Kozlovská (2020) also mentioned that the soundproofing for the magnesium oxide board is quite good, whereby it is good in sound absorption and sound insulation. Furthermore, according to Mokrenko and Kozlovská (2020), the magnesium oxide board also will not undergo deformation, softening, or rot when placed under the influence of moisture or steam.

## **2.10 Summary**

Rubberized lightweight foamed concrete has been evaluated as a core material for a sandwiched wall panel. The review is focused on the engineering properties of rubberized lightweight foamed concrete, including its density, compressive and flexural strength, fire performance, thermal properties, and acoustic properties. In short, rubberized lightweight foamed concrete will show a lower density, and compressive as well as flexural strength but perform better in fire resistance, and acoustic as well as thermal insulation. In addition, the introduction of a magnesium oxide board as the skin layers for sandwiched wall panels also included providing a guideline for the sandwiched wall panel fabrication during the specimen preparation stage.

## CHAPTER 3

### METHODOLOGY AND WORK PLAN

#### 3.1 Introduction

This chapter overviews the methodology for producing rubberized lightweight foamed concrete and sandwiched wall panel as shown in Figure 3.1. First and foremost, the raw materials used in producing the rubberized lightweight foamed concrete and the skin layers for the sandwiched wall panel are introduced. Then, the concrete mixing, casting, and curing processes are described in detail on how to produce the rubberized lightweight foamed concrete. The installation of the skin layer for the sandwiched wall panel is also explained. After the preparation of specimens, product and laboratory tests are conducted, including the acoustic insulation test, fire resistance rating test, and flexural strength test. All tests follow the standard requirements, providing an accurate evaluation of the engineering properties of the sandwiched wall panel.

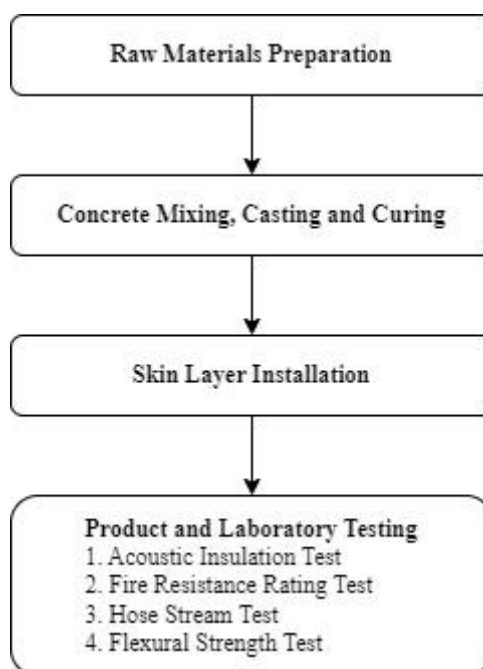


Figure 3.1: Flowchart of Methodology.



## 3.2 Raw Materials Preparation

### 3.2.1 Ordinary Portland Cement

Figure 3.2 shows the cement utilised, Ordinary Portland Cement (OPC), branded as “ORANG KUAT,” manufactured by YTL Cement Sdn. Bhd. The OPC is certified according to MS EN 197-1, CEM 1 52.5. ORANG KUAT is formulated as a high-strength OPC and is anticipated to have easy handling and early de-moulding. Its consistency enhances its suitability for the application of high-strength precast elements. The key benefits of utilising this cement type are high early strength, fast time setting, and consistency in product quality. The general-purpose applications such as precast and brick making are suitable for the ORANG KUAT cement to be utilised. Sieving is required before the concrete mixing. The OPC is required to pass through the size of 600  $\mu\text{m}$  to comply with the standard of ASTM C150. The sieved OPC was placed in an airtight container to prevent the entrant of humid air that will cause the premature hydration process, which will eventually cause the cement to harden as unsuited for further usage.

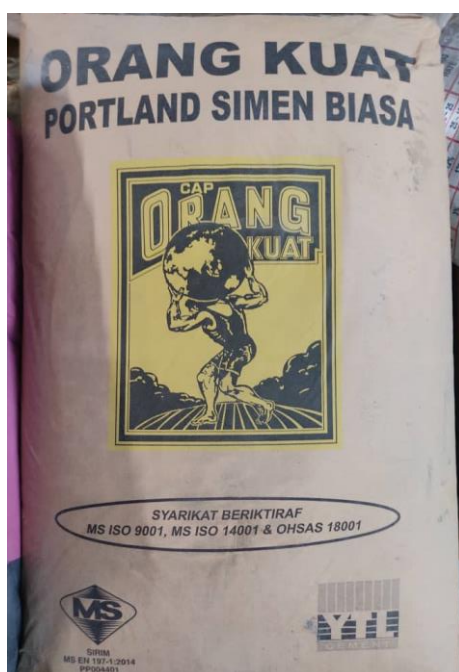


Figure 3.2: ORANG KUAT Ordinary Portland Cement (OPC).

### 3.2.2 Fine Aggregate

The standard taken as reference for the fine aggregate are ASTM C778 and ASTM C136. First and foremost, the fine aggregate was oven-dried at a temperature falling between 100 °C to 110 °C to dry up and remove the excess water content within the aggregate to ensure no extra water would be added to the concrete mixture. After the oven-drying process, the fine aggregate was passed through the sieve analysis process according to ASTM C136. The sieving process could ensure that the fine aggregate size is not more than 600 µm according to the standard specification stated in ASTM C778.

### 3.2.3 Crumb Rubber

The rubber particles used in this study are crumb rubber, as shown in Figure 3.3. The crumb rubber was used to replace part of the proportion of the fine aggregate. In this study, the replacement proportion is 80 %. Furthermore, in terms of the size of the crumb rubber particles, the powdered crumb rubber was used whereby all the powdered crumb rubber passes through the 0.420 mm or named as No. 40 Mesh.



Figure 3.3: Powdered Crumb Rubber.

### **3.2.4 Water**

The standard taken as a reference for the water used throughout the study is ASTM C1602. The water was clear and free from impurities such as acid, alkali, oil, salt, and organic and inorganic products. If any impurities were found in the water, this would affect the concrete properties and thus influence the study's outcome. Furthermore, both potable and non-potable water could be utilised in concrete mixing. Therefore, tap water was used in concrete mixing. In this study, the water-cement ratio used was 0.55. Thus, the water would provide workability to the concrete during the casting process. Besides, it would also result in the cement hydration process, where it reacted with the water and produced the C-S-H gel or calcium silicate hydrate gel.

### **3.2.5 Foaming Agent**

A foaming agent is one of the raw materials for rubberized lightweight foamed concrete. The fresh density for the rubberized lightweight foamed concrete was  $1150 \text{ kg/m}^3$  with a tolerance of  $\pm 50 \text{ kg/m}^3$ . The foam required for the specimen was produced from the foaming agent with the equipment of the foam generator. The foaming agent used was Sika ©Aer 50/50. This product is fulfilling the standard of ASTM C260.

The foam generator consists of numerous parts and sections: the water valve, compressed air valve, inlet and outlet valve, pressure gauge, and the outlet with high-density wire mesh. The main valve is the valve that controls the flow of the compressed air that comes from the compressor. First, a pressure gauge was connected to the main valve to track and control the pressure for the air input. Next, the inlet and outlet valves were attached to the top of the foam generator.

The foaming agent and the water were poured into the foam generator with the mix proportional ratio of 1:20 through the inlet valve for the foam generation process. After that, the air pressure for the foam generator was set as 5 bar or 0.5 MPa. After the pressure was reached, the water and compressed air valve were opened simultaneously to ensure the air and the diluted foam agent could be released together. As a result, the desired foam would come out from the outlet with the high-density tube.

### 3.2.6 Magnesium Oxide Board

The magnesium oxide board was used in this study as the skin layers for the sandwiched wall panel. The thickness of the magnesium oxide board is 9 mm. One specimen contains two pieces of magnesium oxide board to cover both sides. The magnesium oxide board's size is 600 mm × 600 mm, following the size of the rubberized lightweight foamed concrete.

### 3.2.7 TPS Thin Bed Adhesive Premium 668

The TPS Thin Bed Adhesive Premium 668, as shown in Figure 3.4, was utilised in this study. TPS is the adhesive agent connecting the magnesium oxide board and the rubberized lightweight foamed concrete as a sandwiched wall panel. The strong adhesive of the TPS could resist the high temperature so that the wall panel could withstand the high temperature with more than 1000 °C when doing the fire resistance rating test. Besides, the strong adhesive for the TPS could also ensure that the sandwiched wall panel acted as a single integrated structure.



Figure 3.4: TPS Thin Bed Adhesive Premium 668.

### 3.3 Mix Ratio for Rubberized Lightweight Foamed Concrete

Table 3.1 illustrates the materials used to produce the rubberized lightweight foamed concrete. The recipe is also shown in the table with the mix ratio for each type of material. The table serves as a summary and the user guide to produce the rubberized lightweight foamed concrete with a fresh density of 1150 kg/m<sup>3</sup> incorporating 80 % crumb rubber replacement.

Table 3.1: Specimen Mix Ratio.

<b>Materials</b>	<b>Description</b>	<b>Mix Ratio (kg/m<sup>3</sup>)</b>
<b>Cement</b>	Orang Kuat Cement 42.4N - 52.5N	545.39
<b>Sand</b>	Particle size of <600 micrometre	109.08
<b>Water</b>	Usual water supply	299.97
<b>Foam</b>	Sika air entraining agent	14.45
<b>Crumb Rubber</b>	Particle size of 1 to 40 mesh	181.11

### 3.4 Concrete Mixing

Figure 3.5 shows the concrete mixing process. The concrete mixing started with calculating the recipe for each material. The following procedure was weighing the OPC, fine aggregate, and powdered crumb rubber according to the results obtained from the calculation. After that, the dry mixture was prepared whereby the OPC, fine aggregate, and powdered crumb rubber were added to the concrete mixer for the dry mix process until they were mixed well and uniformly. Next, water was added to the dry mixture, where the amount of water needed was calculated based on the weight of the cement added to the mixture. The water-cement ratio was fixed at 0.55. After the water was added, the concrete was mixed well and uniformly. Lastly, the foam was added to the mixture following the foam generation process mentioned in section 3.2.5, and the desired density was 1150 kg/m<sup>3</sup> with a tolerance of  $\pm 50$  kg/m<sup>3</sup>. The amount of foam was added until the density was reached. After the desired concrete density was achieved, the concrete mixing was done, the fresh concrete mixture was produced, and the casting process started.



Figure 3.5: Concrete Mixing Process.

### 3.5 Concrete Casting

Before the concrete casting, the steel mould was checked to ensure no leakage would occur during the concrete pouring. Next, the mould oil was applied to the mould to ease the demoulding process afterwards. Then, the concrete specimen was cast by pouring the fresh concrete mixture into the mould. The mould used was steel mould, and the specimen size was 600 mm × 600 mm × 80 mm. Next, tampering and tapping were applied to ensure the mixture's homogeneity. After that, the trowel was used to flatten the surface of the specimen. After the surface flattening work, the concrete specimen was left for one day for initial hardening. Figure 3.6 shows the concrete casting process.



Figure 3.6: Concrete Casting Process.



### 3.6 Concrete Curing

The cast concrete was placed for initial drying purposes in the steel mould for the first 24 hours. Then, demoulding was performed to obtain the initial hardened concrete specimen from the steel mould. Finally, the water-curing process was conducted continuously for 28 days. The primary purpose of the water curing on the concrete specimen is to ensure the cement within the mixture is fully hydrated, and thus the strength of the concrete could be gained and developed early strength. After 28 days, the specimen could proceed for further action. Figure 3.7 shows the concrete curing process.



Figure 3.7: Concrete Curing Process.

### 3.7 Skin Layer Installation

After the rubberized lightweight foamed concrete was cured for 28 days, the TPS was applied on both side surfaces of the core material, the rubberized lightweight foamed concrete. The scratches were introduced when using the TPS to create the anchorage to increase the adhesiveness between the two related materials: magnesium oxide board and rubberized lightweight foamed concrete. After applying the skin coating on the core materials, one day is required for the TPS hardening. The next day, the TPS was applied on the rough surface of the magnesium oxide board with a thickness of around 3.5 to 4 mm. Consequently, the overall wall panel thickness was controlled at 105 mm.



### 3.8 Acoustic Insulation Test

The standard taken as reference for acoustic insulation test is ISO 10140 – 2: 2010 Acoustics – Laboratory Measurement of Sound Insulation of Building Elements Part 2: Measurement of Airborne Sound Insulation. The test was done in the reverberation room. Two reverberant chambers are interconnected with each other. Chamber 1 is the source room with a total volume of 202.2 m<sup>3</sup> as well as a total surface area of 209 m<sup>2</sup>. Chamber 2 is the room that received the frequency and has a total volume of 268 m<sup>3</sup> and a total surface area of 253 m<sup>2</sup>.

The instruments utilised in this test are B&K Sound Omni-Directional Sound Source - Type 4292-L, B&K Rotating Microphone Boom-Type 3923, Pulse & Classifier Software, B&K Type 3560C Front-end as well as Acoustical Calibrator Rion NC-74 / Gras 42AB. After introducing the instruments used, the testing procedure was installing the test specimen placed in the opening between the two reverberation chambers. After that, a diffuse sound field was generated and evaluated in the source room. The estimation of sound reduction index at a one-third octave centre frequency from 100 Hz to 5000 Hz. The comparison was made between the estimated value for the sound reduction index and the standard reference contour. The result of the comparison is the single-number weighted sound reduction index ( $R_w$ ).

$$R_w = L_1 - L_2 + 10 \log\left(\frac{S}{A}\right) \quad (3.1)$$

where

$R_w$  = single-number weighted sound reduction index, dB

$L_1$  = average sound pressure level in source chamber, dB

$L_2$  = average sound pressure level in receiving chamber, dB

$S$  = area of test specimen, m<sup>2</sup>

$A$  = sound absorption area in receiving chamber, m<sup>2</sup>

### 3.9 Fire Resistance Rating Test

The standards taken as reference for the fire resistance rating test are BS 476: Part 20 – Methods for determination of the fire resistance of elements of construction (general principles) and BS 476: Part 22 – Methods for determination of the fire resistance of non-loadbearing elements of construction.

The specimen was installed into a test frame with the circumstances where one of the vertical edges had been constructed for freedom of movement. The single free-end vertical edge was provided to ensure the specimen was free from the lateral restraint. As a result, the overall test construction size was 3000 mm ( $h$ )  $\times$  3000 mm ( $w$ )  $\times$  105 mm ( $t$ ), excluding the vertical edge gap between the specimen as well as the test frame. The vertical edge gap was filled with ceramic fibre insulation, preventing the hot air from flowing out during the test.

According to section 5 in BS 476: Part 22, the information regarding determining the fire resistance of partitions is shown. For the setting before the test under clause 5.4, examination of the specimen, the furnace control thermocouples should be positioned at least one unit for every area with 1.5 m<sup>2</sup>. The thermocouples should also be away from the furnace for at least 500 mm. Furthermore, the pressuring sensing head should be positioned for at least one unit in the furnace to measure and control the pressure condition within the furnace following the standard. Apart from that, five units of surface temperature measuring thermocouples are positioned at the unexposed side, whereby when is at the centre of the specimen, and the other is placed at the centre of each quarter. Besides, the deflection measuring equipment is used to examine the maximum deflection. However, the deflection position cannot be determined, and thus numerous pieces of equipment are placed in different positions. Therefore, the one reported the maximum values should be taken as maximum deflection. Last but not least, a radiometer is positioned in front of the wall to examine the amount of heat that has been radiated.

Under clause 5.5, the test procedure, the temperature rising should be measured at the unexposed face for both mean and maximum value. Temperature rising is the way to evaluate the insulation properties of the specimen. Besides, the deflection of the specimen should also be monitored, and the maximum deflection should be recorded. According to BS 476: Part 20 clause 9.5.1, the heating should be continued until the failure occurs under the performance criteria as stated or at a time agreed before the heating starts. If the heating process is terminated before the failure occurs, the duration of heating can be taken as the fire resistance time for the specimen.

### **3.10 Hose Stream Test**

The standard taken as reference for the hose stream test is ASTM E2226-10: Standard Practice for Application of Hose Stream. There are two prescriptions which are 207 kPa or 30 psi for water pressure and 2 minutes and 30 seconds for the test duration. Immediately after the fire resistance rating test, the sandwiched wall panel system was moved into the ready position for the hose stream test. The exposed surface of the sandwiched wall panel was subjected to the impact, erosion, as well as cooling effects of a hose stream. On the other hand, the unexposed surface of the sandwiched wall panel was observed during the hose stream was applied. Any hole, crack, or water penetration development from the hose stream should not be found for the sandwiched wall panel to pass the test. The sandwiched wall panel shall be considered to have failed if any developed stream, wetting, water rolling down, and water projected were found at the unexposed surface.

### 3.11 Flexural Strength Test

The standard taken as a reference for the flexural strength test is ASTM C78. The flexural strength test is a three-point load test whereby the loading was applied at the centre of the specimen to determine its flexural strength. The specimen was placed on a roller on each side with a gap of 25 mm from the end edge of the specimen. The support at the specimen on both ends was deemed as pin support. The linear voltage displacement transducer (LVDT) was placed at the bottom side of the specimen to measure the displacement of the specimen after the loading was applied. The LVDT was connected to a data logger for the load-deflection reading generation during the loading-applying process. The load with the increasing rate of 0.5 kN/s was exerted on the middle span of the specimen. The checking was done to ensure the loading applied was in the middle of the specimen for the result accuracy. After all, the setting up and checking were done, the loading was started to be applied to the specimen. The load at which the specimen ruptured in any failure mode was deemed the ultimate flexural or bending strength. Equation 3.2 shows the formula to obtain the modulus of rupture.

$$R = \frac{3PL}{2BD^2} \quad (3.2)$$

where

$R$  = Modulus of Rupture, MPa

$P$  = maximum applied load indicated by the testing machine, kN

$L$  = span length, mm

$B$  = average width of the specimen, mm

$D$  = average depth of specimen, mm

### 3.12 Summary

The two main products produced are the rubberized lightweight foamed concrete and the sandwiched wall panel. The five raw materials, including ordinary Portland cement, fine aggregate, powdered crumb rubber, water, and foam, were prepared well according to the standard requirements for the rubberized lightweight foamed concrete. After that, the concrete mixing was done after the design proportion was calculated with the water-cement ratio of 0.55 and the rubber replacement content of 80 %. The foam was used to ensure the produced rubberized lightweight foamed concrete had a density of 1150 kg/m<sup>3</sup> with a tolerance of  $\pm 50$  kg/m<sup>3</sup>. Next, the concrete was cast into 600 mm  $\times$  600 mm  $\times$  80 mm. After the concrete casting, the specimen was left for 24 hours for the initial hardening of the cement. After 24 hours, the demoulding was done, and the water curing was conducted until the 28<sup>th</sup> day. After the rubberized lightweight foamed concrete was cured, the sandwiched wall panel could proceed to the subsequent product production. First, the TPS was applied on the surface of the specimen with the scratches on it to produce the anchorage for better bonding of the concrete core and the skin layers. After 24 hours, the TPS was applied on the rough surface of the 9 mm thick magnesium oxide board and connected to the concrete core. The skin coat layer was controlled at 4 mm on each side. As a result, the final sizing for the sandwiched wall panel is 600 mm  $\times$  600 mm  $\times$  105 mm. After the specimen preparation, product and laboratory tests, including the acoustic insulation test, fire resistance rating test, and flexural strength test, were conducted in this study.

## CHAPTER 4

### RESULTS AND DISCUSSION

#### 4.1 Introduction

This chapter describes the outcomes and the explanations of four tests conducted to evaluate the sound absorption, 2-hour fire resistance rating, and flexural strength of a sandwiched wall panel system composed of rubberized lightweight foamed concrete with magnesium oxide board as the skin layers. The tests included an acoustic insulation test, fire resistance rating test, hose stream test, and flexural strength test. The quantitative and qualitative results of these product and laboratory tests provide critical information on the sandwiched wall panel system's performance for its industrial application.

The acoustic insulation test utilised the Sound Reduction Index (SRI) parameter to estimate the sandwiched wall panel's sound insulation properties. The test outcomes provide insight into sound transmission loss through the sandwiched wall panel and its executability in noise-reducing.

Fire safety is a critical concern in building design and construction. The 2-hour fire resistance rating test is a standard test method to investigate the ability of building material to maintain its integrity and insulation properties during prolonged fire exposure. The test outcome determines the fire rating of the sandwiched wall panel for its utilisation in the construction industry.

When subjected to high water pressure, the hose stream test evaluated the sandwiched wall panel's resistance to water penetration and structural integrity. This test provides crucial information on the sandwiched wall panel's durability and water resistance ability in adverse conditions.

Modulus of Rupture (MOR) was used to analyse the sandwiched wall panel's flexural strength. MOR measures the maximum stress that a material can withstand before fracturing under bending or axial loading. MOR can provide valuable information to examine the suitability of applying the sandwiched wall panel in the construction industry.

## 4.2 Acoustic Insulation Test

The acoustic insulation test was conducted to obtain the Sound Reduction Index (SRI) parameter. The test commenced after the adhesive agent TPS had undergone an air-curing process. Figures 4.1 and 4.2 illustrate the exposed surface of the sandwiched wall panel at the source room and receiving room, respectively. This study was conducted in compliance with the standard code of ISO 10140-2: 2010. In addition, the standard reference contour for the Sound Reduction Index is also tabulated for comparison with the actual reading obtained from the sandwiched wall panel.



Figure 4.1: Test Setup for Testing of Sandwiched Wall Panel in the Source Room.



Figure 4.2: Test Setup for Testing the Sandwiched Wall Panel in the Receiving Room.

Figure 4.3 and Table 4.1 illustrate the Sound Reduction Index (SRI) and its standard reference at various third-octave centre frequency levels between 100 Hz to 5000 Hz. The SRI tends to fluctuate in the range of third-octave centre frequency from 100 Hz to 250 Hz. However, the standard reference shows a steady upward trend within this frequency range.

In the low-frequency range, the irregular trend causes the SRI of sandwiched wall panel analysis hard to be computed, attributed to the sound waves with lower frequencies having longer wavelengths, causing them to be diffracted to the edges of the sandwiched wall panel. The longer diffracted distance leads to extra transmission loss and fluctuating results. A smaller specimen area might be constructed to reduce the sound wave's diffracted distance, resulting in lower transmission loss and more accurate results. Furthermore, Maurin and Kwapisz (2021) proposed that more octave band frequencies should be adopted to minimise the variations in the low-frequency measurements.

A significant increase was found in sandwiched wall panel's SRI between 315 Hz to 1000 Hz, where it increased from 38.4 dB to 45.6 dB, a difference of 7.2 dB. When compared to the standard reference, the sandwiched



wall panel performed poorer. The standard reference has an SRI of 39.0 dB to 46.0 dB in a similar frequency range, with an overall increase of 7 dB. Although the sandwiched wall panel had a similar increasing rate to the standard reference, the computed SRI at each frequency level was generally lower than the standard reference by an average percentage of 1 %.

When the sandwiched wall panel was exposed to a third-octave centre frequency ranging from 1250 Hz to 5000 Hz, better SRI performance was established in sandwiched wall panel compared with the standard reference. Within the 1250 Hz to 4000 Hz range, SRI ranges from 47.5 dB to 48.1 dB and 47.0 dB for the sandwiched wall panel and standard reference, respectively. The trend in both datasets is toward flattening and remains unchanged except for a minimum fluctuation of less than 1 dB in the actual data set obtained. The sandwiched wall panel shows a higher SRI at each frequency level compared to the standard reference by an average percentage of 1.8 %.

At higher third-octave centre frequencies beyond 4000 Hz, the SRI of sandwiched wall panel continues to show an upward trend while the data flattens out in standard reference. Better performance of sandwiched wall panels is found at higher frequencies than the standard reference. In short, the calculated single-number weighted sound reduction index ( $R_w$ ) utilising equation 3.1 is 43 dB indicating the good sound absorption performance for the sandwiched wall panel as stated by Zhang and Poon (2018).

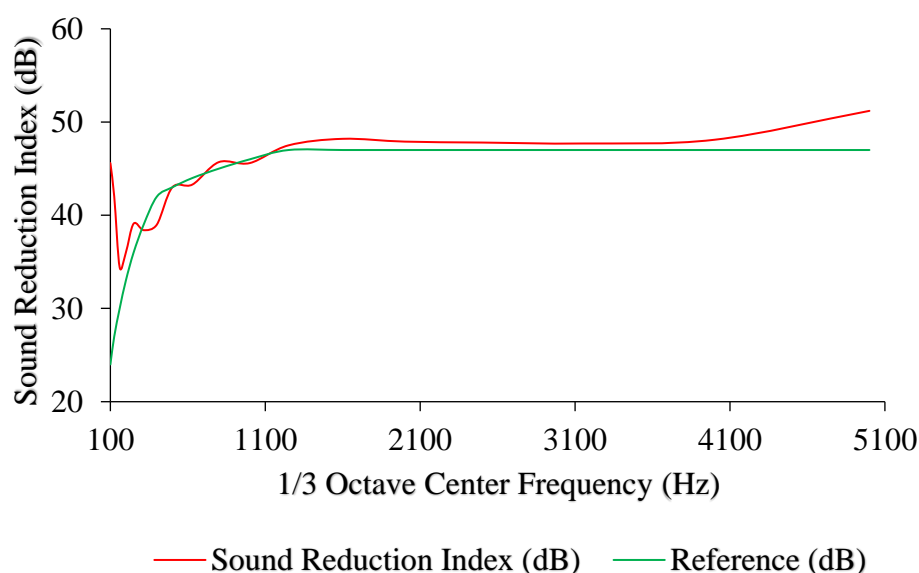


Figure 4.3: Graph on Sound Reduction Index (SRI) versus Frequencies.

Table 4.1: Sound Reduction Index (SRI) at Different Frequencies.

<b>Frequency (Hz)</b>	<b>Sound Reduction Index (dB)</b>	<b>Reference (dB)</b>
<b>100</b>	45.6	24.0
<b>125</b>	42.0	27.0
<b>160</b>	34.4	30.0
<b>200</b>	36.0	33.0
<b>250</b>	39.1	36.0
<b>315</b>	38.4	39.0
<b>400</b>	39.0	42.0
<b>500</b>	43.0	43.0
<b>630</b>	43.3	44.0
<b>800</b>	45.7	45.0
<b>1000</b>	45.6	46.0
<b>1250</b>	47.5	47.0
<b>1600</b>	48.2	47.0
<b>2000</b>	47.9	47.0
<b>2500</b>	47.8	47.0
<b>3150</b>	47.7	47.0
<b>4000</b>	48.1	47.0
<b>5000</b>	51.2	47.0

### **4.3 Fire Resistance Rating Test**

The fire resistance rating test was conducted to examine the integrity and insulation of the sandwiched wall panel. This study complied with British Standards under BS476: Part 22: 1987. The test commenced after the adhesive agent TPS had undergone an air-curing process. Figures 4.4 and 4.6 illustrate the exposed and unexposed faces of the sandwiched wall panel placed in front of the furnace before the fire resistance rating test. On the other hand, Figures 4.5 and 4.7 show the exposed and unexposed faces of the sandwiched wall panel placed in front of the furnace after the fire resistance rating test.

During the fire resistance rating test, the sandwiched wall panel maintained its overall integrity and insulation criterion for the first 30 minutes at the unexposed face. At 35 minutes, a vertical crack was found at the joint near Thermocouple No. 6, which exists from top to bottom of the sandwiched wall panel. At 40 minutes, light smoke started to release from the crack, but the overall sandwiched wall panel maintained its integrity and insulation criterion. Therefore, the sandwiched wall panel maintained its integrity and insulation criterion for the desired test period.

In the fire resistance rating test, both sandwiched wall panels' integrity and insulation properties passed the fire resistance test, which was terminated after 2 hours. Therefore, the test outcomes will be categorised into two categories which are integrity and insulation.



Figure 4.4: The Exposed Face of the Sandwiched Wall Panel Before the Test.



Figure 4.5: The Exposed Face of the Sandwiched Wall Panel After the Test.



Figure 4.6: The Unexposed Face of the Sandwiched Wall Panel Before the Test.



Figure 4.7: The Unexposed Face of the Sandwiched Wall Panel After the Test.



### 4.3.1 Integrity

For the integrity aspect, failure of the specimen will be deemed when the occurrence of specimen collapses, or flame is sustained for more than 10 seconds on the unexposed face. In this study, the sandwiched wall panel eventually sustained its integrity throughout the test.

Apart from qualitative observation, quantitative measurement can also do an integrity check. For example, during the fire resistance rating test, numerous data were taken to comply with the standard requirement. The first information taken was sandwiched wall panel's deflection. The deflection check is significant since the excessive deflection will cause the concrete core to crack and create minor holes within the sandwiched wall panel. In addition, the hot air and flame from the furnace will cause a hike in temperature at the unexposed face, leading to failure.

Furthermore, the excessive deflection will cause the adhesive agent TPS to lose its bonding function. As a result, when the sandwiched wall panel deflected beyond the limit, the centroid of the overall wall panel system will change and become unstable., causing the sandwiched wall panel to lose its integrity and eventually collapse.

Figure 4.8 illustrates the location of points A, B, C, D, and E used to measure the deflection of the sandwiched wall panel. Deflection measurements were taken at these points every 10 minutes throughout the 2-hour test period. Figure 4.9 and Table 4.2 illustrate the deflection at each point at a 10-minute interval during the test period. The positive value shown in Table 4.2 indicates the deflection occurred at the sandwiched wall panel moving towards the direction of the furnace; meanwhile, the negative value indicates the circumstance of the sandwiched wall panel's deflection moving away from the furnace. In this study, all the deflection measured was moved towards the furnace.

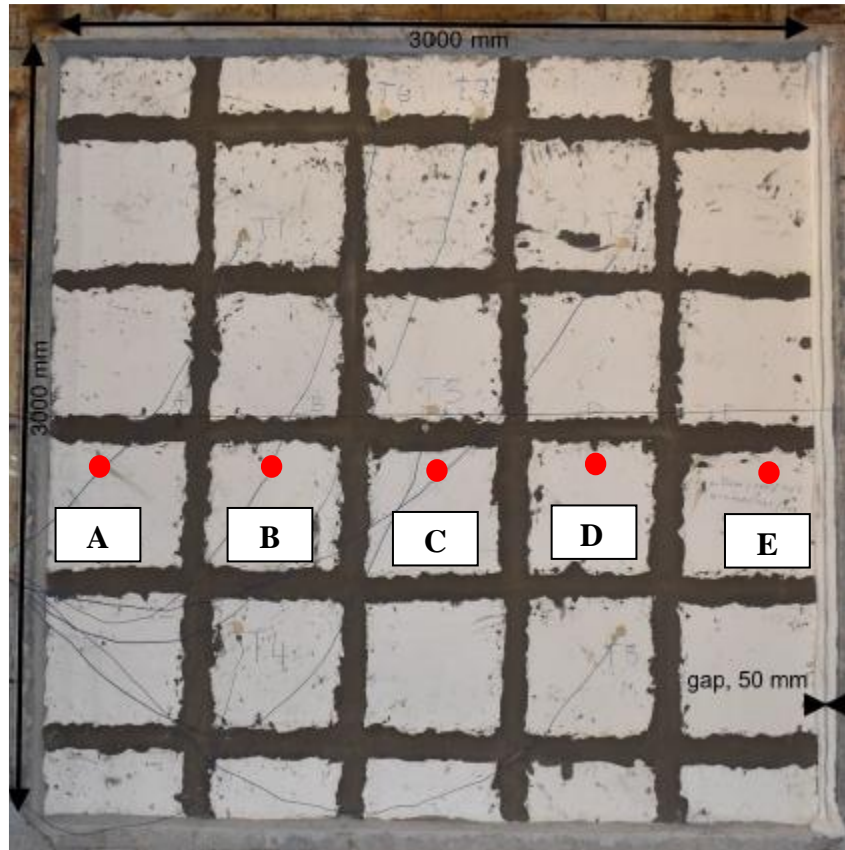


Figure 4.8: Location of Points A to E for Deflection Measuring.

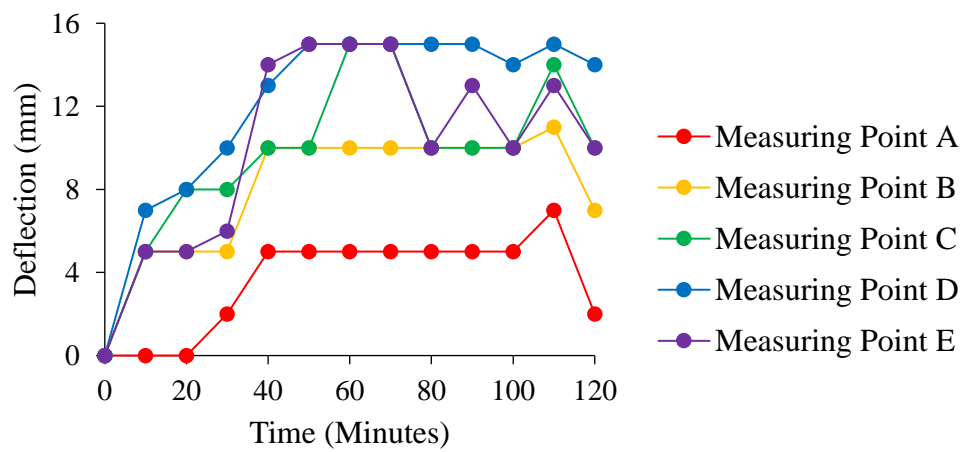


Figure 4.9: Graph on Deflection versus Time at Five Measuring Points.

Table 4.2: Deflection Measured at Five Measuring Points.

Time (Mins)	Measuring Points				
	A (mm)	B (mm)	C (mm)	D (mm)	E (mm)
<b>0</b>	0	0	0	0	0
<b>10</b>	0	5	5	7	5
<b>20</b>	0	5	8	8	5
<b>30</b>	2	5	8	10	6
<b>40</b>	5	10	10	13	14
<b>50</b>	5	10	10	15	15
<b>60</b>	5	10	15	15	15
<b>70</b>	5	10	15	15	15
<b>80</b>	5	10	10	15	10
<b>90</b>	5	10	10	15	13
<b>100</b>	5	10	10	14	10
<b>110</b>	7	11	14	15	13
<b>120</b>	2	7	10	14	10

Table 4.2 provides information on the deflection measurement of the sandwiched wall panel during the fire resistance rating test. The highest deflection recorded within the 2-hour fire resistance rating test is 15 mm. The maximum allowable deflection limit for a non-load-bearing precast lightweight wall panel is typically determined as  $L/180$ , whereas  $L$  is the span length of the wall panel in the unit of millimetres. In compliance with Uniform Building By-Laws 1984 (UBBL), the maximum allowable deflection limit is calculated as 16.7 mm. Figure 4.9 reveals a significant rise in deflection at 40 minutes, coinciding with the observation of a vertical crack at 35 minutes. This can be attributed to the crack allowing the high-temperature atmosphere in the furnace to penetrate through the sandwiched wall panel, resulting in further deflection.

The deflection during the fire resistance rating test is attributable to the differential pressure between the furnace and the atmosphere. The elevated temperature within the furnace space will cause the particles to move faster and create more space, reducing the inner pressure. As a result, the pressure in the atmosphere is greater than in the furnace, pushing the sandwiched wall panel



toward the furnace space. Although the fixed end condition of the sandwiched wall panel restrains the pressure from the atmosphere, the restriction will gradually reduce from the edge to the centre of the sandwiched wall panel. As such, the critical deflection of the sandwiched wall panel will occur in the middle. Consequently, the deflection check is located near the midsection of the sandwiched wall panel.

In addition, relatively minor deflection observed in the sandwiched wall panel can be attributed to the concrete core construction method. The concrete cores were arranged and stacked together using the stretcher bond arrangement, as illustrated in Figure 4.10. The stretcher bond allows for a faster construction speed and ensures that the concrete cores are integrated. As a result, the separated concrete core will experience deflection individually, and the overall sandwiched wall panel's deflection can be minimised. This is attributable to each concrete core can resist the load independently without transmitting to each other.

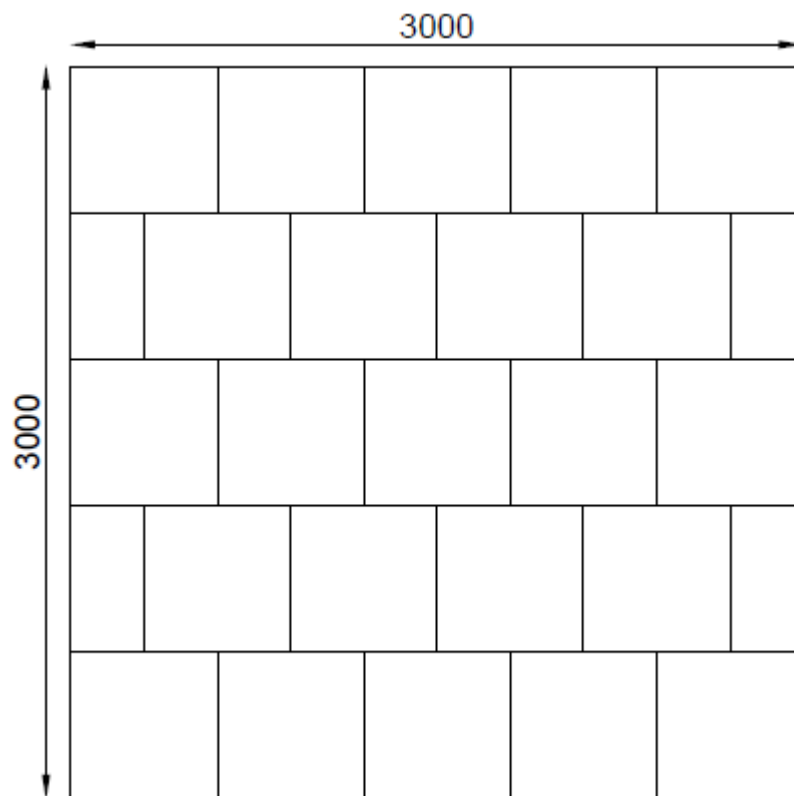


Figure 4.10: General Arrangement of the Concrete Core.

The Magnesium Oxide boards were bonded to the concrete core using TPS adhesive with a specific arrangement, as illustrated in Figure 4.11. The cross arrangement was applied to both sides of the concrete core, and the Magnesium Oxide boards were arranged in a cross mode against the inner concrete core. This arrangement enhances the bonding effect within the overall sandwiched wall panel. In addition, the separated Magnesium Oxide boards, which are 600 mm  $\times$  600 mm, allow each board to deflect independently instead of acting as a single large element of 3000 mm  $\times$  3000 mm.

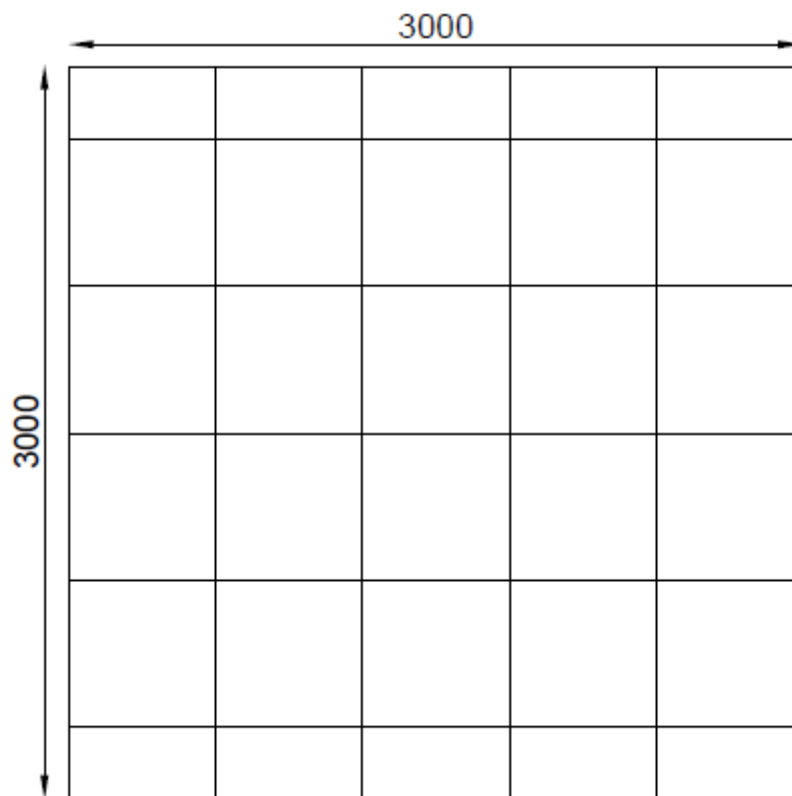


Figure 4.11: General Arrangement of the Magnesium Oxide Board.

### 4.3.2 Insulation

For the insulation aspect, the specimen's insulation property was also tested during the fire resistance test. The failure of the test shall be deemed when the mean temperature at the unexposed specimen face is inclined to more than 140 °C from the start or the temperature measured at any location of the unexposed specimen face is inclined to more than 180 °C from the mean value of initial temperature at unexposed face. The specimen shall be declared a pass in the fire resistance test when no failure was deemed during the test period.

The information taken to evaluate the insulation property is the temperature at the unexposed surface of the sandwiched wall panel. The temperature captured at the unexposed surface of the sandwiched wall panel was recorded by seven thermocouples named T1 to T7 attached at different positions, as shown in Figure 4.12.

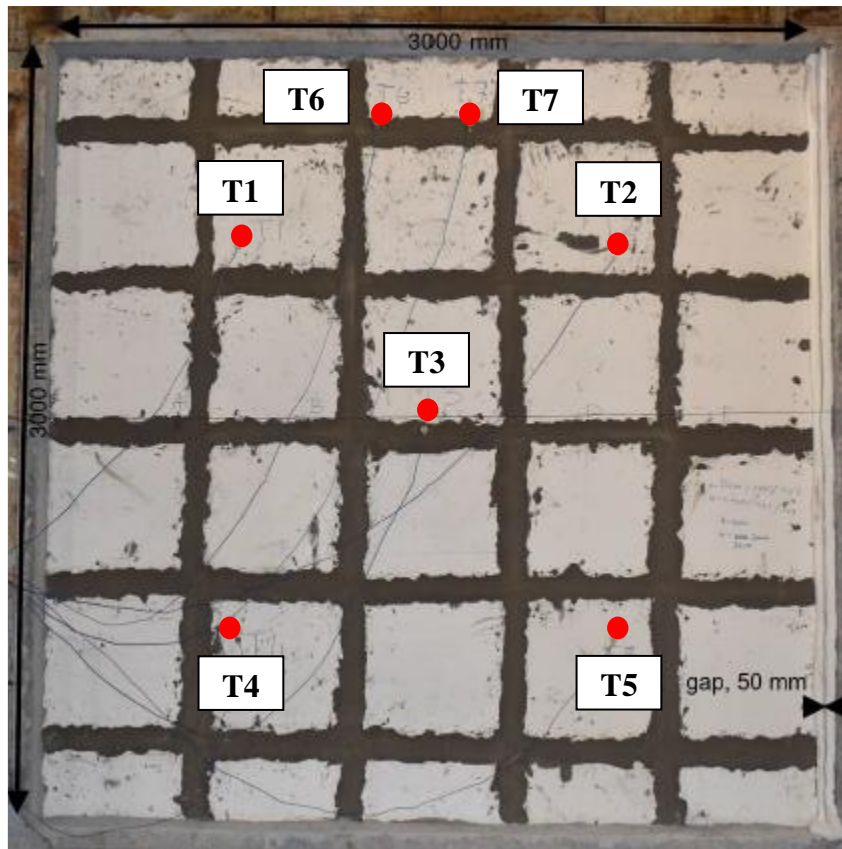


Figure 4.12: Location of Thermocouple No.1 to 7.

The results of the temperature measurement taken by the seven thermocouples located at the unexposed surface of the sandwiched wall panel are presented in Figure 4.13 and Table 4.3. The initial mean temperature recorded immediately after the start of the test was 29 °C, and it remained constant for the first 30 minutes of the test. After 40 and 50 minutes, the mean temperature increased to 30 °C and 31 °C, respectively. Subsequently, the mean temperature increased by 2 °C every 10 minutes at 60 and 70 minutes, resulting in mean temperatures of 33 °C and 35 °C, respectively. Beyond 70 minutes, the mean temperature increased at 4 °C every 10 minutes until the test was terminated. Finally, the mean temperature reached 55 °C at the end of the 2-hour test.

The mean temperature of sandwiched wall panel exhibited a gradual increase from 29 °C to 33 °C in the first hour of the test and sharply rose from 33 °C to 55 °C during the second hour. The rate of increase was 4 °C and 22 °C in the first and second halves of the test, respectively. It should be noted that the rate of the mean temperature changes during the second-hour testing was significantly higher than that observed in the first hour. The abrupt increase in temperature was likely due to the formation of a vertical crack line in the sandwiched wall panel at 35 minutes. The crack allowed the hot gases from the furnace to flow out and caused the unexposed surface of the sandwiched wall panel to become higher temperature. All temperature readings remained at 29 °C in the first half an hour of the test before the crack line formation.

Before the crack line formation, the sandwiched wall panel blocked the heat transfer by radiation inside the furnace to the unexposed surface. The heat transfer was only done by conduction through the sandwiched wall panel. The low thermal conductivity of the magnesium oxide board, adhesive agent TPS, and rubberized lightweight foamed concrete reduced the heat conduction rate, resulting in good heat insulation properties.

However, after the crack line formation, the atmosphere inside the furnace could flow out, allowing the heat transfer by radiation from the furnace to the unexposed surface of the sandwiched wall panel. The crack line acted as a medium for the hot gases inside the furnace to flow out and come into contact with the unexposed surface of the sandwiched wall panel. Consequently, the

insulation performance of the sandwiched wall panel was compromised due to the crack line formation.

Crack line formation allows the hot gases inside the furnace to flow out, causing the higher temperature detected at the unexposed surface of the sandwiched wall panel. The quantitative data of the temperature taken at Thermocouples No. 3 and No. 6 is consistent with the observation since they are located close to the crack line and thus experience a higher temperature increase. This phenomenon shows the importance of maintaining the integrity of the sandwiched wall panel during a fire. This is attributable to the tiny cracks or minor openings affecting the wall panel's insulation properties.

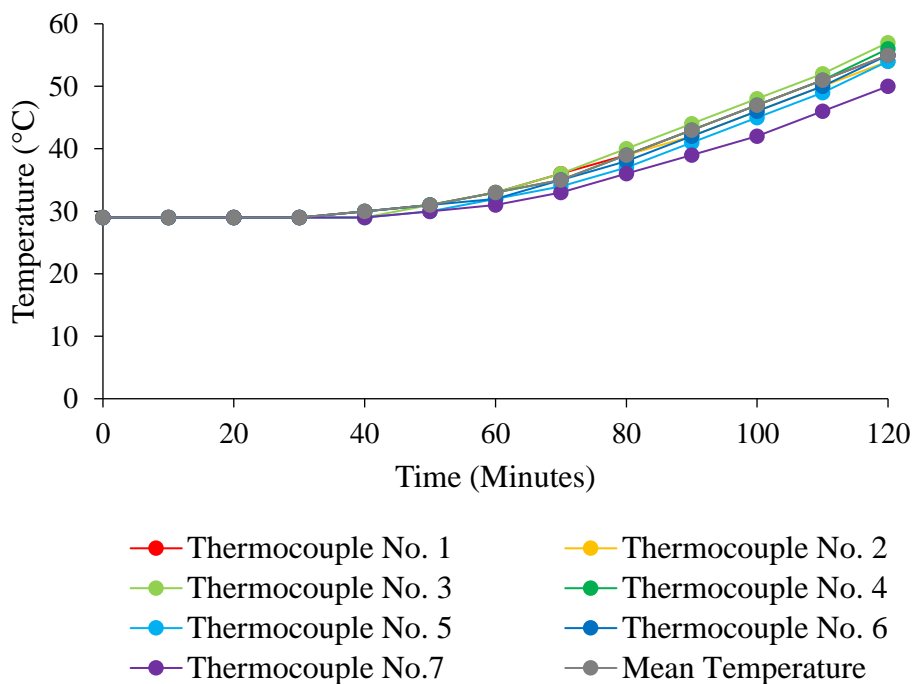


Figure 4.13: Graph on Temperature versus Time at Seven Thermocouples.

Table 4.3: Temperature Measured at Seven Thermocouples.

Time (Mins)	Thermocouple No.							Mean Temp. (°C)
	T1	T2	T3	T4	T5	T6	T7	
	(°C)	(°C)	(°C)	(°C)	(°C)	(°C)	(°C)	
<b>0</b>	29	29	29	29	29	29	29	29
<b>10</b>	29	29	29	29	29	29	29	29
<b>20</b>	29	29	29	29	29	29	29	29
<b>30</b>	29	29	29	29	29	29	29	29
<b>40</b>	30	30	29	30	29	30	29	30
<b>50</b>	31	31	31	31	30	31	30	31
<b>60</b>	33	33	33	33	32	32	31	33
<b>70</b>	36	35	36	35	34	35	33	35
<b>80</b>	39	39	40	39	37	38	36	39
<b>90</b>	43	42	44	43	41	42	39	43
<b>100</b>	47	46	48	47	45	46	42	47
<b>110</b>	51	50	52	51	49	50	46	51
<b>120</b>	55	54	57	56	54	55	50	55

Figures 4.14 and 4.15 illustrate the temperature trends of the sandwiched wall panel during a fire resistance test. The mean and maximum temperature increases were recorded at 10-minute intervals. Two significant threshold values were established to determine the temperature rise from the initial values, namely 140 °C and 180 °C for the mean and maximum temperature values, respectively. The highest mean and maximum temperature increase were below the threshold values, measuring 24 °C and 26 °C, respectively. The temperature rises in both cases was significantly lower than the thresholds, indicating that the sandwiched wall panel can withstand fire exposure for a longer time, more than 2 hours.

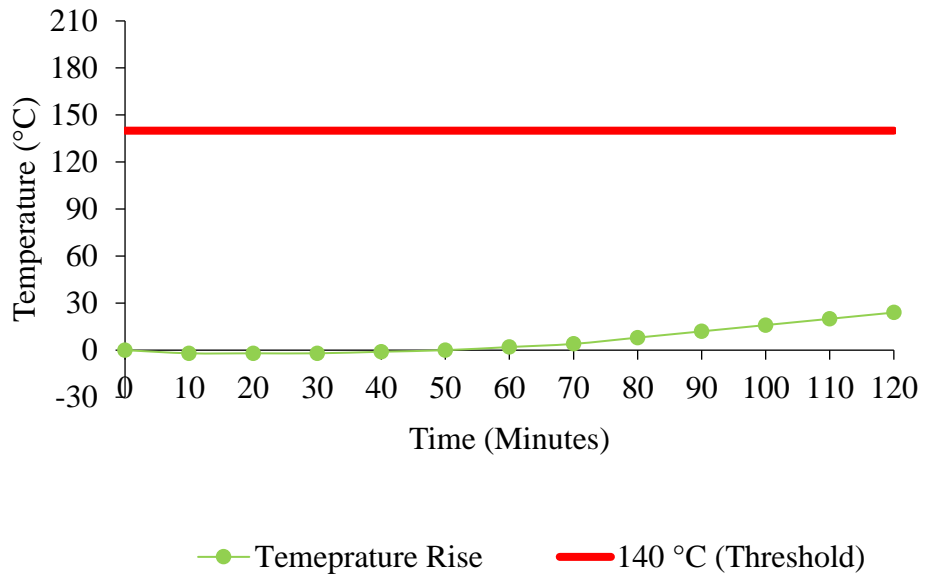


Figure 4.14: Graph on Rise in Mean Temperature versus Time.

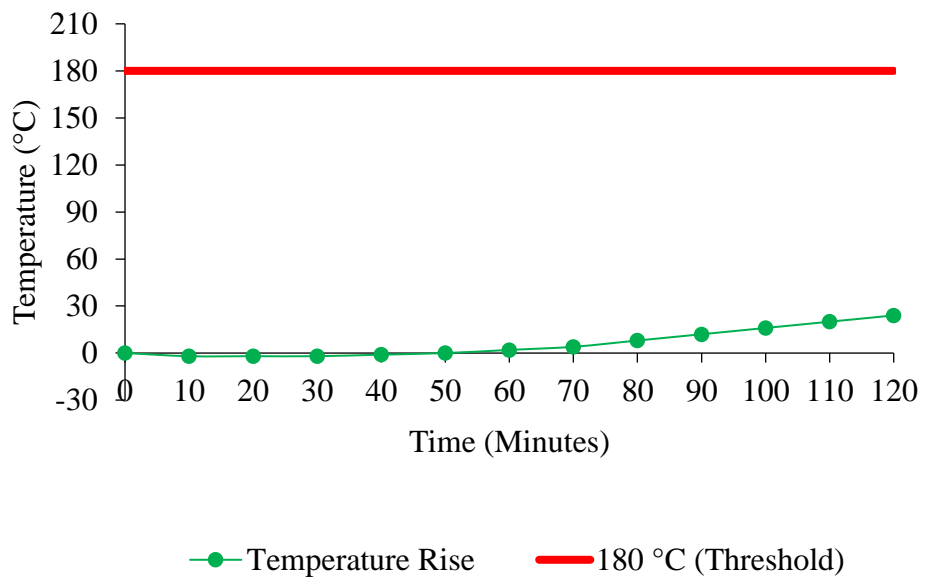


Figure 4.15: Graph on Rise in Maximum Temperature versus Time.

Table 4.4: Temperature Rise at the Unexposed Surface at a 10-minute Interval.

<b>Time (Minutes)</b>	<b>Temperature Rise Above Initial Mean Temperature</b>	
	<b>Mean</b>	<b>Maximum</b>
	<b>Temperature (°C)</b>	<b>Temperature (°C)</b>
<b>0</b>	0	-2
<b>10</b>	-2	-2
<b>20</b>	-2	-2
<b>30</b>	-2	-2
<b>40</b>	-1	-1
<b>50</b>	0	0
<b>60</b>	2	2
<b>70</b>	4	5
<b>80</b>	8	9
<b>90</b>	12	13
<b>100</b>	16	17
<b>110</b>	20	21
<b>120</b>	24	26

The initial negative value recorded during the first 40 minutes of the fire resistance rating test is attributed to the sandwiched wall panel's excellent thermal insulation properties. The high temperature in the inner furnace cannot efficiently transfer the heat to the unexposed surface of the sandwiched wall panel. Additionally, the unexposed surface faces the atmosphere, an uncontrollable environment subjected to random temperature changes influenced by the weather or wind speed. The thermocouples may capture these fluctuations and impact the result's accuracy. After 40 minutes, the temperature rise becomes a positive value attributed to the crack line formation in the sandwiched wall panel. At this time, the temperature inside the furnace reaches up to 1000 °C. The random temperature change of 1 to 2 °C no longer significantly affects the temperature change as the cracked line formed compromised the sandwiched wall panel's excellent insulation property.



#### 4.4 Hose Stream Test

The hose stream test is critical, followed by the fire resistance rating test. This test determines the specimen's ability to withstand the water spurred from the hose stream that passes through it. The hose stream test is failed if any opening that allows water to project beyond the unexposed surface is developed within the specified time. The duration of the hose stream test is typically 2.5 minutes or 150 seconds, and the water is pressurized up to 207 kPa or 30 psi.

Figure 4.16 illustrates the exposed surface of the sandwiched wall panel after completing the hose stream test. The sandwiched wall panel with a core of rubberized lightweight foamed concrete and the skin layers of magnesium oxide board could withstand the hose stream test within 2.5 minutes. Although the skin layer was flushed away due to the high-water pressure, no crack or hole development allows water penetration to the unexposed surface. The sandwiched wall panel remained intact and maintained its integrity. Thus, it passes the hose stream test.

The success of the sandwiched wall panel in passing the hose stream test can be attributed to several factors:

- (i) The excellent bonding adhesive agent and construction workmanship filled all the gaps and holes within the rubberized lightweight foamed concrete cores. This prevented water leaks to the unexposed surface.
- (ii) The rubberized lightweight foamed concrete cores are arranged in stretcher bonds providing a typical block construction that enhances the overall integrity of the wall panel system.
- (iii) When applying high-water pressure, the one free vertical edge of the sandwiched wall panel system reduced moment and torsion.

In short, the sandwiched wall panel could pass the hose stream test due to the excellent workmanship, correct adhesive agent selection, and application of stretcher bond for concrete core construction. These elements ensure that it is executable in a building application.



Figure 4.16: The Exposed Face of the Specimen after the Hose Stream Test.

The hose stream test is a critical evaluation for the sandwiched wall panel system to be commonly used in the construction industry. Due to the vertical orientation of wall panels, they partition and separate large building spaces for multiple uses. In the event of a fire breakout, firefighters require high water pressure from a hose stream to control and extinguish the fire. Suppose the sandwiched wall panel fails to sustain its integrity and remains intact after undergoing the hose stream test. In that case, it can result in significant danger of financial loss during firefighting efforts. This is attributed to the wall panel collapsing when subjected to high water pressure, obstructing the escape route and potentially trapping and burying victims within the fire scene. Therefore, a wall panel that passes the hose stream test is essential to ensure the safety of building occupants and firefighters.

#### 4.5 Flexural Strength Test

The flexural strength test was carried out on a sandwiched wall panel that had undergone air curing and had been bonded using a TPS adhesive agent between the core of rubberized lightweight foamed concrete and the skin layers of magnesium oxide board. The test was conducted with the sandwiched wall panel placed horizontally, and the load was applied at a rate of 0.5 kN/s until the sandwiched wall panel failed. The actual set-up of the overall testing before the load was applied is illustrated in Figure 4.17. The load applied, and the sandwiched wall panel deflected at the failure point were recorded during the test.



Figure 4.17: Actual Set-up of Flexural Strength Test.

When the load exceeded the maximum load capacity, the sandwiched wall panel cracked and ruptured in the middle portion, as seen in Figure 4.18. The effective bonding effect from TPS demonstrated well element connection within the core of rubberized lightweight foamed concrete, the skin layers of magnesium oxide board, and the adhesive agent of TPS, ensuring they crack simultaneously. TPS acted as an intermediate medium to transfer the internal forces between elements within the sandwiched wall panel. As the load applied approached the element's modulus of rupture (MOR), the excessive load was transferred to the other to prevent the overall sandwiched wall panel from rupturing. Eventually, when the loading bearing capacity of all elements was exceeded, the failure occurred. The sandwiched wall panel cracked, crushed, and collapsed.



Figure 4.18: Specimen's Condition at Ultimate Failure.

Figure 4.19 and Table 4.5 present the load-deflection curve for the sandwiched wall panel. From the curve, the maximum load applied to it is 19.68 kN, and its maximum deflection is 0.9150 mm. A steeper slope of the graph was observed from zero loading to 5 kN loading. This trend indicated the presence of voids within the sandwiched wall panel. This causes smaller deflection since the loading on it compresses the void until all the elements within the sandwiched wall panel are fully bonded. The load-deflection curve increases at 0.016 mm/kN within the first 5 kN loading and approximately 0.05 mm/kN beyond. Beyond the 5 kN, the load-deflection curve shows an approximately constant trend and slope until the maximum load is applied. Deflection beyond the maximum loading applied is not included since the sandwiched wall panel was crushed and collapsed.

Using Equation 3.2, the Modulus of Rupture (MOR) of the sandwiched wall panel computed is 2.2313 MPa. MOR measures the ultimate strength of the sandwiched wall panel subjected to a bending load before rupturing. During the flexural strength test, an axial force is applied on the upper surface of the specimen, causing compressive stress to be exerted on the upper surface and tensile stress to be exerted at the lower surface. Therefore, MOR can aid in determining the ability of the sandwiched wall panel to resist such pressures and indicate its overall flexural strength.

In Malaysia, the standard for minimum MOR for precast lightweight concrete wall panels used in non-load-bearing walls is set by MS 72: 1972: Part 2. The standard states that the minimum MOR requirement is 1.5 MPa. The sandwiched wall panel in this study surpassed the minimum requirement with a MOR of 2.2313 MPa. Therefore, it can be concluded that this sandwiched wall panel suites for non-load-bearing walls under the Malaysia Standard.

The relatively low MOR found in this study is likely attributed to the absence of reinforcing steel or wire mesh embedded within the concrete core. Concrete is known to perform well when encountering compressive stress but can perform poorly when facing tensile stress. Thus, the concrete core can withstand high tensile stress with reinforcing steel and eventually will crack and collapse. Reinforcing steel or wire mesh can significantly increase the sandwiched wall panel's tensile strength and MOR.

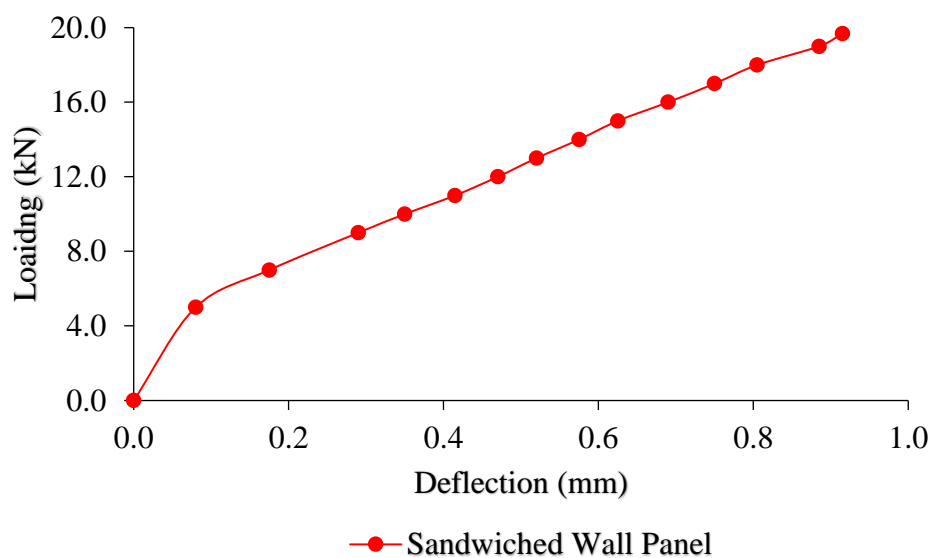


Figure 4.19: Load-deflection Curve for Sandwiched Wall Panel.

Table 4.5: Load-deflection Information for Sandwiched Wall Panel.

<b>Loading (kN)</b>	<b>Deflection (mm)</b>
<b>0.00</b>	0.0000
<b>5.00</b>	0.0800
<b>7.00</b>	0.1750
<b>9.00</b>	0.2900
<b>10.00</b>	0.3500
<b>11.00</b>	0.4150
<b>12.00</b>	0.4700
<b>13.00</b>	0.5200
<b>14.00</b>	0.5750
<b>15.00</b>	0.6250
<b>16.00</b>	0.6900
<b>17.00</b>	0.7500
<b>18.00</b>	0.8050
<b>19.00</b>	0.8850
<b>19.68</b>	0.9150

#### **4.6 Summary**

This chapter reveals the comprehensive results obtained from the acoustic insulation test, fire resistance rating test, hose stream test, and flexural strength test for the full-scale rubberized lightweight foamed concrete with magnesium oxide board as the skin layers. The acoustic insulation test revealed a Sound Reduction Index (SRI) of 43 dB, indicating that the sandwiched wall panel can reduce the noise or sound by 43 dB as the sound wave passes.

The fire resistance rating test and hose stream test were conducted to investigate the integrity and thermal insulation of the sandwiched wall panel. The sandwiched wall panel could sustain itself without any severe crack or deformation during the high-temperature fire test for 2 hours and the high-pressure water test for 2.5 minutes. In addition, it demonstrated good performance when encountering adverse conditions.

The flexural strength test yielded a Modulus of Rupture (MOR) of 2.2313 MPa for the sandwiched wall panel, which is considered acceptable for a non-load-bearing wall panel system since the sandwiched wall panel can support its weight without collapsing and fulfil the Malaysia Standard of MS 72: 1972: Part 2 simultaneously.

The full-scale rubberized lightweight foamed concrete with magnesium oxide board as the skin layers is deemed to have good sound reduction performance, fire resistance performance, and the good structural performance of a wall panel system.

## CHAPTER 5

### CONCLUSIONS AND RECOMMENDATIONS

#### 5.1 Conclusions

In conclusion, the sandwiched wall panel with the core of rubberized lightweight foamed concrete, the skin layers of magnesium oxide board, and the adhesive agent of TPS have resulted in the development of eco-friendly and energy-efficient buildings. The study revealed that the rubberized lightweight foamed concrete core had a fresh density of 1150 kg/m<sup>3</sup> with 80 % crumb rubber replacement. The study mainly focused on sound absorption, fire resistance rating, and flexural strength evaluation, which is crucial for precast wall panels to fulfil the standard requirement.

The first objective of this study is to study the sound absorption of the sandwiched wall panel in different levels of the third-octave centre frequency. The acoustic insulation test indicated that the full-scale rubberized lightweight foamed concrete with magnesium oxide board as the skin layers had a good sound absorption quality with a weighted Sound Reduction Index (SRI) of 43 dB in the frequency range of 100 Hz to 5000 Hz.

The second objective of this study is to investigate the 2-hour fire resistance rating of the sandwiched wall panel. The fire resistance rating test and the hose stream test confirmed that the full-scale rubberized lightweight foamed concrete with magnesium oxide board as the skin layers maintained its integrity and insulation properties and remained intact even after the 2-hour fire exposure 2.5-minute hose stream test.

The third objective of this study is to evaluate the flexural strength of the sandwiched wall panel. A test was conducted to obtain the maximum axial load applied and the maximum deflection observed before it cracked and crushed. The Modulus of Rupture (MOR) of the full-scale rubberized lightweight foamed concrete with the magnesium oxide board as the skin layers was revealed as 2.2313 MPa, exceeding the standard requirement of 1.5 MPa for a non-load-bearing wall panel system.



## 5.2 Recommendations for future work

This report only focuses on sound absorption, fire resistance rating, and flexural strength of the full-scale rubberized lightweight foamed concrete with the magnesium oxide board as the skin layers. However, these are the fundamental properties for immediate industrial application, but further information for the sandwiched wall panel needs to be covered. Hence, an in-depth study should be carried out regarding the other engineering properties of the sandwiched wall panel and the actual impact on the use of the rubberized lightweight foamed concrete in the construction industry. Here are some recommendations for future work:

- (i) Evaluate the thermal conductivity of the full-scale rubberized lightweight foamed concrete with the magnesium oxide board as the skin layers. This data can function as dedicated support for decision-making on selecting the sandwiched wall panel to be utilised in a green building.
- (ii) Study on the impact of the sandwiched wall panel on the environment. The study may cover the carbon footprint, which this study still needs to assess. The carbon footprint is a significant element in evaluating the eco-friendliness of the sandwiched wall panel.
- (iii) Investigate the feasibility of other incorporating types of waste materials into the rubberized lightweight foamed concrete core for better engineering performance and alternate skin layer selection for better insulation.

## REFERENCES

- Bharath, M., Saravanan, J., Sha, A.K., Ghimire, B.R., Bhagat, K., Sherstha, L., Ghimire, P., Kasaudhan, R., Sha, S. and Madhu, S., 2022. Novel sandwich structure approach to develop lightweight concrete canoe. *Materials Today: Proceedings*, [e-journal] 65(2), pp.1779–1784. <https://doi.org/10.1016/j.matpr.2022.04.801>.
- Bing, C. and Ning, L., 2014. Experimental Research on Properties of Fresh and Hardened Rubberized Concrete. *Journal of Materials in Civil Engineering*, [e-journal] 26(8), pp.1–8. [https://doi.org/10.1061/\(asce\)mt.1943-5533.0000923](https://doi.org/10.1061/(asce)mt.1943-5533.0000923).
- Carsana, M., Tittarelli, F. and Bertolini, L., 2013. Use of no-fines concrete as a building material: Strength, durability properties and corrosion protection of embedded steel. *Cement and Concrete Research*, [e-journal] 48, pp.64–73. <https://doi.org/10.1016/j.cemconres.2013.02.006>.
- Chiaro, G., Palermo, A., Granello, G., Tasalloti, A., Stratford, C. and Banasiak, L., 2019. Eco-rubber seismic-isolation foundation systems: a cost-effective way to build resilience. *2019 Pacific Conference on Earthquake Engineering*, [online] Available at < <https://www.researchgate.net/publication/332342810> > [Accessed 7 September 2022].
- De Maeijer, P. K., Craeye, B., Blom, J. and Bervoets, L., 2021. Crumb Rubber in Concrete—The Barriers for Application in the Construction Industry. *Infrastructures*, [e-journal] 6(8). <https://doi.org/10.3390/infrastructures6080116>.
- Elshazly, F., Mustafa, S. and Fawzy, H., 2020. Rubberized concrete properties and its structural engineering applications – An overview. *Egyptian Journal for Engineering Sciences and Technology*, [e-journal] 30, pp.1–11. <https://doi.org/10.21608/eijest.2020.35823.1000>.
- Eltayeb, E., Ma, X., Zhuge, Y., Xiao, J. and Youssf, O., 2022. Composite walls Composed of profiled steel skin and foam rubberized concrete subjected to eccentric compressions. *Journal of Building Engineering*, [e-journal] 46(1). <https://doi.org/10.1016/j.jobe.2021.103715>.
- Fawzy, H.M., Mustafa, S.A.A. and Elshazly, F.A., 2020. Rubberized concrete properties and its structural engineering applications-An overview. *The Egyptian International Journal of Engineering Sciences and Technology*, [online] Available at: <<https://ejest.journals.ekb.eg/>> [Accessed 28 July 2022].
- Fiore, A., Marano, G.C., Marti, C. and Molfetta, M., 2014. On the Fresh/Hardened Properties of Cement Composites Incorporating Rubber Particles from Recycled Tires. *Advances in Civil Engineering*, [e-journal] 2014. <https://doi.org/10.1155/2014/876158>.

Ganjian, E., Khorami, M. and Maghsoudi, A.A., 2009. Scrap-tyre-rubber replacement for aggregate and filler in concrete. *Construction and Building Materials*, [e-journal] 23(5), pp.1828–1836. <https://doi.org/10.1016/j.conbuildmat.2008.09.020>.

Hasanbeigi, A., Price, L. and Lin, E., 2012. Emerging energy-efficiency and CO<sub>2</sub> emission-reduction technologies for cement and concrete production: A technical review. *Renewable and Sustainable Energy Reviews*, [e-journal] 16(8), pp.6220–6238. <https://doi.org/10.1016/j.rser.2012.07.019>.

Ismail, K.M., Fathi, M.S. and Manaf, M.B., 1997. First report research project on lightweight concrete. 71908(2), pp.35–43.

Jiahao, L., Chin Lian, F., Hejazi, F. and Azline, N., 2019. Study of properties and strength of no-fines concrete. *IOP Conference Series: Earth and Environmental Science*, [e-journal] 357. <https://doi.org/10.1088/1755-1315/357/1/012009>.

Jin, H., Yin, D. and Yu, S., 2022. Mesoscale research on electric potential of rubberized concrete affected by rubber geometry. *Construction and Building Materials*, [e-journal] 340. <https://doi.org/10.1016/j.conbuildmat.2022.127851>.

Kashani, A., Ngo, T.D., Mendis, P., Black, J.R. and Hajimohammadi, A., 2017. A sustainable application of recycled tyre crumbs as insulator in lightweight cellular concrete. *Journal of Cleaner Production*, [e-journal] 149, pp.925–935. <https://doi.org/10.1016/j.jclepro.2017.02.154>.

Kumar, S., Chen, B., Xu, Y. and Dai, J.G., 2021. Structural behavior of FRP grid reinforced geopolymer concrete sandwich wall panels subjected to concentric axial loading. *Composite Structures*, [e-journal] 270. <https://doi.org/10.1016/j.compstruct.2021.114117>.

Lim, Z.H., Lee, F.W., Mo, K.H., Kwong, K.Z. and Yew, M.K., 2020. The Influence of Powdered Crumb Rubber on the Mechanical Properties and Thermal Performance of Lightweight Foamed Concrete. *IOP Conference Series: Materials Science and Engineering*, [e-journal] 739. <https://doi.org/10.1088/1757-899X/739/1/012016>.

Ling, T.C., 2011. Prediction of density and compressive strength for rubberized concrete blocks. *Construction and Building Materials*, [e-journal] 25(11), pp.4303–4306. <https://doi.org/10.1016/j.conbuildmat.2011.04.074>.

Maurin, A. and Kwapisz, L., 2021. Simplified method for calculating airborne sound transmission through composite barriers. *Composite Structures*, [e-journal] 276. <https://doi.org/10.1016/j.compstruct.2021.114526>.

Mokrenko, D. and Kozlovská, M., 2020. Comparative analysis of magnesium oxide boards properties. *IOP Conference Series: Materials Science and Engineering*, [e-journal] 867. <https://doi.org/10.1088/1757-899X/867/1/012032>.

- Narayanan, N. and Ramamurthy, K., 2000. Structure and properties of aerated concrete: A review. *Cement and Concrete Composites*, [e-journal] 22(5), pp.321–329. [https://doi.org/10.1016/S0958-9465\(00\)00016-0](https://doi.org/10.1016/S0958-9465(00)00016-0).
- Ng, S.C., Low, K.S. and Tioh, N.H., 2011. Newspaper sandwiched aerated lightweight concrete wall panels - Thermal inertia, transient thermal behavior and surface temperature prediction. *Energy and Buildings*, [e-journal] 43(7), pp.1636–1645. <https://doi.org/10.1016/j.enbuild.2011.03.007>.
- Nor, N.S.M. and Ishak, Y.M., 2016. The Effect of Various Sizes of Waste Tyre Rubber Shred on Concrete Strength. [online] Available at: <[https://www.researchgate.net/publication/298134137\\_THE\\_EFFECT\\_OF\\_VARIOUS\\_SIZES\\_OF\\_WASTE\\_TYRE\\_RUBBER\\_SHRED\\_ON\\_CONCRETE\\_STRENGTH](https://www.researchgate.net/publication/298134137_THE_EFFECT_OF_VARIOUS_SIZES_OF_WASTE_TYRE_RUBBER_SHRED_ON_CONCRETE_STRENGTH)>
- Othuman, M.A. and Wang, Y.C., 2011. Elevated-temperature thermal properties of lightweight foamed concrete. *Construction and Building Materials*, [e-journal] 25(2), pp.705–716. <https://doi.org/10.1016/j.conbuildmat.2010.07.016>.
- Panesar, D.K., 2013. Cellular concrete properties and the effect of synthetic and protein foaming agents. *Construction and Building Materials*, [e-journal] 44, pp.575–584. <https://doi.org/10.1016/j.conbuildmat.2013.03.024>.
- Parhi, P.S., 2015. Scrap-Tyre-Rubber Replacement for Aggregate in Cement Concrete: Experimental Study. *International Journal of Earth Sciences and Engineering*, [online] Available at: <[https://www.researchgate.net/publication/272019232\\_Scrap-Tyre-Rubber\\_Replacement\\_for\\_Aggregate\\_in\\_Cement\\_Concrete\\_Experimental\\_Study](https://www.researchgate.net/publication/272019232_Scrap-Tyre-Rubber_Replacement_for_Aggregate_in_Cement_Concrete_Experimental_Study)> [Accessed 6 September 2022].
- Pereira, D., Gago, A., Proenca, J. and Morgado, T., 2016. Fire performance of sandwich wall assemblies. *Composites Part B: Engineering*, [e-journal] 93, pp.121–131. <https://doi.org/10.1016/j.compositesb.2016.03.001>.
- Pham, T.M., Liu, J., Tran, P., Pang, V.L., Shi, F., Chen, W., Hao, H. and Tran, T.M., 2020. Dynamic compressive properties of lightweight rubberized geopolymer concrete. *Construction and Building Materials*, [e-journal] 265. <https://doi.org/10.1016/j.conbuildmat.2020.120753>.
- Rusthi, M., Ariyanayagam, A., Mahendran, M. and Keerthan, P., 2017. Fire tests of Magnesium Oxide board lined light gauge steel frame wall systems. *Fire Safety Journal*, [e-journal] 90, pp.15–27. <https://doi.org/10.1016/j.firesaf.2017.03.004>.
- Sayadi, A.A., Tapia, J. V., Neitzert, T.R. and Clifton, G.C., 2016. Effects of expanded polystyrene (EPS) particles on fire resistance, thermal conductivity and compressive strength of foamed concrete. *Construction and Building Materials*, [e-journal] 112, pp.716–724. <https://doi.org/10.1016/j.conbuildmat.2016.02.218>.

Sofi, A., 2018. Effect of waste tyre rubber on mechanical and durability properties of concrete – A review. *Ain Shams Engineering Journal*, [e-journal] 9(4), pp.2691–2700. <https://doi.org/10.1016/j.asej.2017.08.007>.

Sukontasukkul, P., 2009. Use of crumb rubber to improve thermal and sound properties of pre-cast concrete panel. *Construction and Building Materials*, [e-journal] 23(2), pp.1084–1092. <https://doi.org/10.1016/j.conbuildmat.2008.05.021>.

Szydłowski, R. and Mieszcak, M., 2017. Study of Application of Lightweight Aggregate Concrete to Construct Post-tensioned Long-span Slabs. *Procedia Engineering*, [e-journal] 172, pp.1077–1085. <https://doi.org/10.1016/j.proeng.2017.02.166>.

Thienel, K.C., Haller, T. and Beuntner, N., 2020. Lightweight concrete-from basics to innovations. *Materials*, [e-journal] 13(5). <https://doi.org/10.3390/ma13051120>.

Thomas, B.S., Gupta, R.C. and Panicker, V. J., 2015. Experimental and modelling studies on high strength concrete containing waste tyre rubber. *Sustainable Cities and Society*, [e-journal] 19, pp.68–73. <https://doi.org/10.1016/j.scs.2015.07.013>.

Wang, G., Zhang, B., Shui, Z., Tang, D. and Kong, Y., 2012. Experimental study on the performance and microstructure of rubberized lightweight aggregate concrete. *Progress in Rubber, Plastics and Recycling Technology*, [e-journal] 28(4), pp.147–156. <https://doi.org/10.1177/147776061202800401>.

Wang, R., Gao, P., Tian, M. and Dai, Y., 2019. Experimental study on mechanical and waterproof performance of lightweight foamed concrete mixed with crumb rubber. *Construction and Building Materials*, [e-journal] 209, pp.655–664. <https://doi.org/10.1016/j.conbuildmat.2019.03.157>.

Zhang, B. and Poon, C.S., 2018. Sound insulation properties of rubberized lightweight aggregate concrete. *Journal of Cleaner Production*, [e-journal] 172, pp.3176–3185. <https://doi.org/10.1016/j.jclepro.2017.11.044>.

Zheng, L., Huo, X.S. and Yuan, Y., 2008. Strength, Modulus of Elasticity, and Brittleness Index of Rubberized Concrete. *Journal of Materials in Civil Engineering*, [e-journal] 20(11), pp.692–699. [https://doi.org/10.1061/\(asce\)0899-1561\(2008\)20:11\(692\)](https://doi.org/10.1061/(asce)0899-1561(2008)20:11(692)).

Zhu, H. and Carlson, D.D., 1999. Spray based crumb rubber technology in highway noise reduction application. *Proceedings of the International Conference on Solid Waste Technology and Management*, pp.815–822.